The Astronomical Journal, 164:196 (21pp), 2022 November https://doi.org/10.3847/1538-3881/ac9126

Joint Constraints on Exoplanetary Orbits from Gaia DR3 and Doppler Data

Joshua N. Winn
Department of Astrophysical Sciences, Princeton University, Princeton, NJ 08544, USA
Received 2022 August 11; revised 2022 September 6; accepted 2022 September 10; published 2022 October 17

Abstract

The third Gaia data release includes a catalog of exoplanets and exoplanet candidates identified via the star's astrometric motion. This paper reports on tests for consistency between the Gaia two-body orbital solutions and precise Doppler velocities for stars currently amenable to such a comparison. For BD-17 0063, HD 81040, and HD 132406, the Gaia orbital solution and the Doppler data were found to be consistent and were fitted jointly to obtain the best possible constraints on the planets' orbits and masses. Inconsistencies were found for four stars: HD 111232, probably due to additional planets that were not included in the astrometric model; HD 175167 and HR 810, possibly due to inaccurate treatment of non-Gaussian uncertainties in the Gaia orbital solutions; and HIP 66074, for unknown reasons. Consistency tests were also performed for HD 114762, which was reported in 1989 to have a brown dwarf or exoplanet but has since been shown to be a binary star. The joint Gaia–Doppler analysis shows the secondary mass to be $0.215 \pm 0.013\,M_{\odot}$ and the orbital inclination to be $3\overset{\circ}{.}63 \pm 0\overset{\circ}{.}06$.

Unified Astronomy Thesaurus concepts: Exoplanet astronomy (486); Extrasolar gaseous giant planets (509); Exoplanets (498); Astrometry (80); Radial velocity (1332); Orbit determination (1175)

1. Introduction

The astrometric technique for exoplanet detection is based on sensing a star's reflex motion projected onto the sky plane. It is the oldest method for generating exoplanet candidates (see, e.g., Strand 1943) and has recently returned to prominence, thanks to data from Gaia Collaboration et al. (2022a). As part of Data Release 3 (DR3), Holl et al. (2022) presented a catalog of candidate exoplanets that includes 73 astrometric detections.

The astrometric method for planet detection is important because it can reveal all of a planet's orbital parameters and uniquely specify its mass (see, e.g., Quirrenbach 2010). However, despite the unprecedented precision of Gaia astrometry, the current data are only sensitive to giant planets, and even then, the signal-to-noise ratios are typically modest ($\sim$10). With current Doppler spectrographs, giant planets can be detected with much higher signal-to-noise ratios, but the Doppler data do not reveal the orbital inclination and give only a lower limit on the planet's mass. Thus, the two techniques are complementary.

Gaia Collaboration et al. (2022b) highlighted 11 astrometrically detected exoplanets for which high-precision Doppler data are already available and compared the published Doppler-based values of the orbital period and eccentricity with the values determined by Gaia. The good matches served to validate the methods that were used to derive orbital parameters from the Gaia astrometry, although the team also noted some discrepancies. In keeping with the desire for the initial DR3 publications to be based solely on Gaia data as much as possible, the Gaia team did not perform joint fitting of the astrometric and Doppler data. Doing so would allow for a more thorough evaluation of the consistency between the two data sets and would also provide the best possible constraints on the planets' masses and orbital parameters. That was the purpose of the work described in this paper.

While analyzing the planet-hosting stars, the opportunity was also taken to revisit HD 114762b, the erstwhile exoplanet candidate discovered by Latham et al. (1989). Astrometric data from Gaia have already shown that the orbit is viewed nearly face on and that the companion's mass exceeds the minimum mass of a star (Kiefer 2019; Holl et al. 2022), but the results of a joint Gaia–Doppler fitting have not yet been reported.

This paper is organized as follows. Section 2 introduces the sample of stars, Section 3 explains the methods of analysis, and Section 4 describes the results. The results are briefly summarized and discussed in Section 5.

2. Sample Selection

A straightforward approach to determining the orbital parameters would be to fit a two-body model to the combination of radial-velocity and astrometric time-series data. However, the Gaia time-series astrometric data have not yet been released. Instead, DR3 provides a summary of the results of fitting a two-body model to the astrometric time-series data. This information is sufficient for present purposes, but only when the star's radial-velocity variations and astrometric motion are both dominated by the effect of a single planet. When multiple planets make detectable contributions to the star's motion, the results of a two-body fit are difficult to interpret, at best, and meaningless, at worst. Therefore, the list of stars to be analyzed was restricted to those for which which useful Doppler data are available, and only a single giant planet has been reported.

This narrowed down the list to seven stars (in addition to the special case of HD 114762, described above). For one of those stars, HIP 66074, Gaia astrometry triggered the initial detection of the planet, although a small amount of precise radial-velocity data had previously been obtained as part of a Doppler survey. For the other six stars, BD-17 0063, HD 81040, HD 132406, HD 111232, HR 810, and HD 175167, the planet was initially discovered via the Doppler method. The stars that needed to be rejected on account of having multiple known companions were HD 142 (Wittenmyer et al. 2012), HD 164604 (Arriagada et al. 2010), and GJ 876 (Marcy et al. 2001). Another star, HIP 28193,

Table 1
Sources of Radial-velocity Data

Star Name	Instrument Name	# of RVs	Median unc. (m s^{-1})	Time Span (days)	Time Range (year/month)	Reference
BD-17 0063	HARPS	26	1.5	1760	2003/10–2008/08	Moutou et al. (2009)
HD 81040	ELODIE	23	12	1210	2002/02–2005/05	Sozzetti et al. (2006)
HD 81040	HIRES	3	12	254	1999/04–2000/01	Sozzetti et al. (2006)
HD 132406	ELODIE	17	11	748	2004/05–2006/06	da Silva et al. (2007)
HD 132406	SOPHIE	4	4	150	2006/12–2007/05	da Silva et al. (2007)
HIP 66074	HIRES	10	1.5	1399	2009/04–2013/02	Butler et al. (2017)
HR 810	UCLES	25	4.7	2458	1998/10–2005/07	Butler et al. (2017)
HR 810	CES	95	17	1977	1992/11–1998/04	Kürster et al. (2000)
HR 810	CORALIE	26	9	604	1998/07–2000/03	Naef et al. (2001)
HR 810	HARPS	47	2.0	717	2003/11–2005/10	Trifonov et al. (2020)
HD 175167	MIKE	13	4.2	1828	2004/07–2009/07	Arriagada et al. (2010)
HD 111232	MIKE	15	3.2	1326	1998/02–2001/10	Minniti et al. (2009)
HD 111232	CORALIE	38	5.5	1181	2000/03–2003/06	Mayor et al. (2004)
HD 111232	HARPS	58	2.0	4489	2004/02–2016/05	Trifonov et al. (2020)
HD 114762	HJS/Coudé	86	34	591	1988/11–1990/07	Cochran et al. (1991)
HD 114762	Hamilton[a]	74	22	6900	1990/03–2009/02	Kane et al. (2011)
HD 114762	HIRES	24	1.7	2039	2013/12–2019/07	Rosenthal et al. (2021)

Notes. For comparison, the Gaia observations that are the basis of DR3 took place over about 1038 days, between 2014 July 25 and 2017 May 28 (Gaia Collaboration et al. 2022a).
[a] The dewar for the Hamilton spectrograph was changed six times over the time span of the observations. Each dewar change was regarded as a change of spectrograph, introducing another offset and jitter parameter.

was excluded because the available radial-velocity data are sparse and affected by stellar activity (Holl et al. 2022).

Table 1 gives a summary of the Doppler data gathered from the literature. The results of the two-body fits to the Gaia data were obtained from the `gaiadr3.nss_two_body_orbits` table at the Gaia archive.[1] The `gaiadr3.astrophysical_parameters` table (Creevey et al. 2022) was also consulted to obtain the stellar properties determined by the General Stellar Parametrizer from Spectroscopy (`gspspec`) and Photometry (`gspphot`), as well as the stellar mass from the Final Luminosity Age Mass Estimator (FLAME).

3. Methods

For each star, there were three stages in the analysis. First, the Doppler data were fitted alone (Section 3.1). Second, the Gaia data were fitted alone, or to be more precise, the tabulated results of the two-body fit were used to determine the posterior probability distributions for the parameters that are independently constrained by the Doppler data (Section 3.2). Third, the Doppler and Gaia results were compared in detail (Section 3.3). If they were consistent, then a joint fit was performed. The results for individual stars are described in Section 4.

3.1. Doppler Analysis

The Doppler data are in the form of one or several time series of radial-velocity measurements $v(t_i)$ and associated uncertainties σ_i, with each series coming from a different telescope and spectrograph. They were modeled with the radial-velocity equation,

$$v(t) = K\{\cos[f(t) + \omega] + e\cos\omega\} + \gamma, \quad (1)$$

where K is the radial-velocity semiamplitude, e is the orbital eccentricity, $f(t)$ is the true anomaly, ω is the argument of pericenter, and γ is the time-independent component of the radial-velocity data (either the actual radial velocity of the center of mass or, more typically, an arbitrary radial velocity associated with the template spectrum from which relative radial velocities were determined). Given the time of a measurement, the true anomaly was calculated from t_p and e by iteratively solving Kepler's equation for the eccentric anomaly $E(t)$,

$$\frac{2\pi}{P}(t - t_p) = E(t) - e\sin E(t) \quad (2)$$

and then calculating

$$f(t) = 2\tan^{-1}\left[\sqrt{\frac{1+e}{1-e}}\tan\frac{E(t)}{2}\right]. \quad (3)$$

The Doppler likelihood function $\mathcal{L}_v$ was taken to be

$$\mathcal{L}_v = \prod_{i=1}^{N}\frac{1}{\sqrt{2\pi(\sigma_{v,i}^2 + \sigma_0^2)}}\exp\left[-\frac{(v_i - v_{i,\rm calc})^2}{2(\sigma_{v,i}^2 + \sigma_0^2)}\right], \quad (4)$$

where i runs over all the data points, $v_{i,\rm calc}$ is the calculated velocity based on a given choice of model parameters, v_i is the measured radial velocity, $\sigma_{v,i}$ is the formal uncertainty, and σ_0 is the "velocity jitter," a constant meant to account for unmodeled systematic errors.

Posterior sampling was performed with the Monte Carlo Markov Chain algorithm of Goodman & Weare (2010) as implemented by the code `emcee` (Foreman-Mackey et al. 2013).[2] The "stepping parameters" in the chain were

$$\{K,\ \sqrt{e}\cos\omega,\ \sqrt{e}\sin\omega,\ P,\ t_p\}, \quad (5)$$

[1] https://gea.esac.esa.int/archive/

[2] Here and elsewhere, the number of "walkers" was 32, and the number of "links" was chosen to be 500,000, which was always more than 50 times the integrated autocorrelation length for each parameter.

along with the nuisance parameters γ and σ_0 specific to the data from each spectrograph. Thus, for a case in which all the data were from a single spectrograph, the total number of parameters was seven. Each additional spectrograph increased the number of parameters by two. Uniform priors were adopted for each stepping parameter.

3.2. Gaia Analysis

The traditional or "Campbell" orbital elements are

$$\{a, e, I, \omega, \Omega, P, t_p\}, \tag{6}$$

where a is the semimajor axis, I is the inclination, and Ω is the longitude of the ascending node. The Gaia DR3 results are expressed in a different basis,

$$\{A, B, F, G, e, P, t_p\}, \tag{7}$$

where A, B, F, and G are the angular Thiele–Innes coefficients, defined as

$$A = a_0(\cos\omega\cos\Omega - \sin\omega\sin\Omega\cos I), \tag{8}$$

$$B = a_0(\cos\omega\sin\Omega + \sin\omega\cos\Omega\cos I), \tag{9}$$

$$F = -a_0(\sin\omega\cos\Omega + \cos\omega\sin\Omega\cos I), \text{ and} \tag{10}$$

$$G = -a_0(\sin\omega\sin\Omega - \cos\omega\cos\Omega\cos I). \tag{11}$$

In these definitions, a_0 is the semimajor axis of the observed orbit converted into angular units by multiplying by the parallax, ϖ. For a star with a dark companion, such as a planet, the observed orbit is the star's orbit. When the light from the companion is not negligible, the observed orbit is that of the "photocenter" (the apparent position of the unresolved combination of light from both bodies), a point discussed further in Section 3.3.

The Gaia team determined the orbital elements by fitting a model to the Gaia time-series astrometric data that also included parameters for the position, proper motion, and parallax. The `gaiadr3.nss_two_body_orbits` table contains a list of best-fit parameters and a correlation matrix, which was converted into a covariance matrix $\boldsymbol{C}$ using the `nsstools` code[3] (Halbwachs et al. 2022). The Gaia likelihood function $\mathcal{L}_g$ was taken to be

$$\mathcal{L}_g = \frac{1}{\sqrt{(2\pi)^8|\det \boldsymbol{C}|}}\exp\left[-\frac{1}{2}(\boldsymbol{\Theta}^T\boldsymbol{C}^{-1}\boldsymbol{\Theta})^2\right], \tag{12}$$

where $\boldsymbol{\Theta}$ is the "Gaia deviation vector," an eight-element column vector composed of differences between the Gaia-measured values and the calculated values for the seven parameters given in Equation (7) and the parallax.

The Gaia likelihood was used to produce samples from the posterior probability density for the parameters

$$\{a_0, e, \cos I, \omega, \Omega, P, t_p, \varpi\}. \tag{13}$$

Uniform priors were employed for these parameters, and the `emcee` code was used for sampling. At each step in the chain, these parameters were used to compute A, B, F, and G, thereby allowing $\boldsymbol{\Theta}$ to be constructed and the likelihood to be evaluated.

[3] https://www.cosmos.esa.int/web/gaia/dr3-nss-tools

3.3. Joint Analysis

At this stage, a comparison was made between the Doppler and Gaia-based results for the set of parameters they have in common:

$$\{e, \omega, P, t_p\}. \tag{14}$$

For the t_p parameter, the Gaia convention was followed, in which t_p refers to the orbit that was underway at epoch 2016.0 (JD 2,457,389.0) and takes values between $-P/2$ and $+P/2$. In addition, the Doppler results for K were compared to the radial-velocity semiamplitude implied by the Gaia parameters (assuming the light from the companion is negligible),

$$K = \frac{2\pi}{P}\frac{(a_0/\varpi)\sqrt{1-\cos^2 I}}{\sqrt{1-e^2}}. \tag{15}$$

If the parameters were inconsistent, an attempt was made to ascertain the reason, as described in the next section on a case-by-case basis. If they were consistent, then a joint fit was performed.

The model parameters for the joint fit were

$$\{M, m, \sqrt{e}\cos\omega, \sqrt{e}\sin\omega, \cos I, \Omega, P, t_p, \varpi, \varepsilon\} \tag{16}$$

along with the nuisance parameters γ and σ_0 for each spectrograph. A Gaussian prior was placed on the primary mass M based on the value from the `gaiadr3.astrophysical_parameters` table, or from the literature, as described below. The secondary mass m was subject to a uniform prior, as were all the other parameters. The ε parameter is the flux ratio between the companion and the primary star. The flux ratio is relevant because, as noted earlier, Gaia measures the motion of the center of light of the star and any unresolved companions. Thus, strictly speaking, the reported orbital parameters pertain to the "photocenter" and not the star. For a given choice of model parameters, a_0 was computed using the equation

$$\frac{a_0}{\varpi} = [G(M+m)]^{1/3}\left(\frac{P}{2\pi}\right)^{2/3}\left(\frac{m}{M+m} - \frac{\varepsilon}{1+\varepsilon}\right), \tag{17}$$

which is based on Kepler's third law and the assumption that the photocenter is the flux-weighted mean position of the two bodies. Once a_0 is determined, the Thiele–Innes coefficients can be computed, the Gaia deviation vector $\boldsymbol{\Theta}$ can be constructed, and the likelihood $\mathcal{L}_g$ can be evaluated.

Although the correction for ε is important for binary stars, we expect it to be negligible ($\ll 10^{-4}$) for planets and brown dwarfs. For example, according to Table 5 of the compilation of stellar properties by Pecaut & Mamajek (2013; as updated on the website of E. Mamajek[4]), a solar-mass star with an $0.08\,M_\odot$ companion would have a Gaia-band flux ratio of about 4×10^{-5}. This allowed the ε parameter to serve as another consistency check: If the companion is a planet or brown dwarf and the Gaia and Doppler data are consistent, then the credible interval for ε should encompass values smaller than 10^{-4}. Because of this firm expectation, whenever the data were found to be consistent with a completely dark companion, the joint fit was repeated with the additional constraint $\varepsilon = 0$. The intention

[4] https://www.pas.rochester.edu/~emamajek/EEM_dwarf_UBVIJHK_colors_Teff.txt

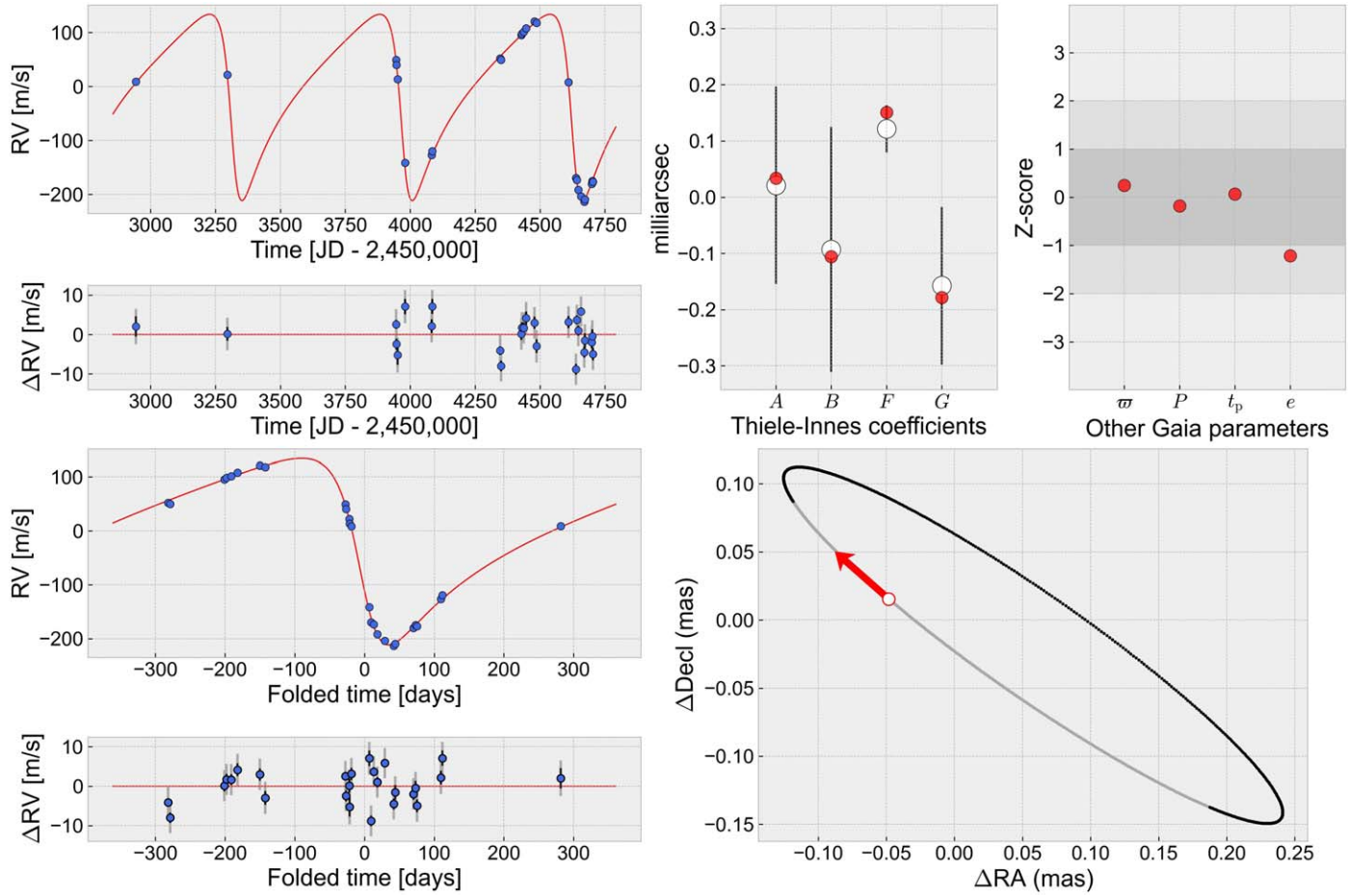

Figure 1. BD-17 0063: results of the joint Gaia–Doppler fit, assuming the companion is dark. Left: Doppler data as a function of time and folded time, with residuals. Red curves show the maximum a posteriori probability (MAP) model. Right: The two top panels compare the parameters of the joint model with those from Gaia alone. The first panel shows the Thiele–Innes coefficients; open symbols are the Gaia-only values and red points are from the MAP model. The second panel shows the *Z*-score ("number of sigma") between the Gaia-only and best-fit parameters. The lower-right panel shows the orbital geometry according to the MAP model, with black representing the portion on the "near side" of the sky plane and gray representing the "far side." The origin is the location of the center of mass, the white circle marks the pericenter position, and the red arrow conveys the direction of motion.

was to avoid biasing the results by allowing unrealistically large flux ratios.

4. Results

4.1. BD-17 0063

BD-17 0063 (HIP 2247) is a K dwarf at a distance of 35 pc with a Gaia optical apparent magnitude of $G = 9.2$. Moutou et al. (2009) discovered a giant planet around this star. They determined the star's mass to be $0.74 \pm 0.04\,M_{\odot}$ (the value adopted here) and reported the planet's minimum mass, period, and eccentricity to be 5.1 Jupiter masses, 655.6 days, and 0.54, respectively. Judging from the literature, the planet has not received much attention since its discovery.

Although the available radial velocities span three planetary orbits, most of the data were obtained during a single orbit. The Doppler-only analysis showed that the spectroscopic orbit is well constrained, with the strongest covariances seen between P and t_p, and between $\sqrt{e}\cos\omega$ and $\sqrt{e}\sin\omega$.

The Doppler data and Gaia two-body orbital solution for this system are harmonious. The Doppler-only results for K, P, t_p, e, and ω all agree to within 1.5σ with the Gaia-only results. The Doppler-only results are more precise. For example, the K value is 172.5 ± 1.6 m s^{-1} based only on radial velocities and 147^{+45}_{-24} m s^{-1} based on the Gaia orbital solution.

The joint fit was successful, providing a good match to all of the radial velocities and the parameters of the Gaia two-body orbital solution. The flux ratio was found to be compatible with zero, with an upper bound of 0.18% with 95% confidence—another sign of concordance between the data sets. For this reason, the joint fit was repeated with the constraint $\varepsilon = 0$. The quality of the fit can be assessed in Figure 1, which shows the radial-velocity data as a function of both time and phase (left), the level of agreement with the Gaia orbital solution (upper right), and the orbital geometry (lower right). For this system and the others, Table 2 gives the results of the joint fit, and the Appendix contains a "corner plot" showing the two-dimensional posterior probability distributions for each pair of parameters, marginalized over all the others. In the joint fit, the orbit is inclined by $81° \pm 4°$, the planet's mass is 5.16 ± 0.20 Jupiter masses, and the eccentricity is $e = 0.5439 \pm 0.0052$.

4.2. HD 81040

HD 81040 (HIP 46076) is a G star at 34 pc with $G = 7.6$. According to the Gaia team's FLAME, the star's mass is $0.962 \pm 0.040\,M_{\odot}$. Sozzetti et al. (2006) discovered a giant

Table 2
Results of Jointly Fitting the Gaia and Doppler Data

Parameter	BD-17 0063	HD 81040	HD 132406	HIP 66074[a]	HD 175167[b]
M [$M_\odot$]	0.741 ± 0.040	0.962 ± 0.040	0.973 ± 0.040	0.671 ± 0.050	1.090 ± 0.040
m [$M_{\rm Jup}$]	5.16 ± 0.20	7.53 ± 0.032	$5.94^{+0.65}_{-0.59}$	$0.445^{+0.055}_{-0.046}$	$14.8^{+1.8}_{-1.6}$
P [days]	655.57 ± 0.58	1004.7 ± 3.0	908 ± 16	300.3 ± 1.3	1175 ± 25
$t_{\rm p}$ [days]	-138.5 ± 2.8	126 ± 17	-225 ± 69	52 ± 14	-194 ± 73
e	0.5439 ± 0.0052	$0.527^{+0.034}_{-0.037}$	$0.250^{+0.063}_{-0.075}$	0.418 ± 0.067	0.510 ± 0.035
$\cos I$	0.149 ± 0.069	$-0.366^{+0.077}_{-0.071}$	$-0.64^{+0.11}_{-0.09}$	$-0.030^{+0.077}_{-0.081}$	0.814 ± 0.023
ω [rad]	1.987 ± 0.031	1.275 ± 0.075	4.18 ± 0.22	4.56 ± 0.018	$5.75^{+0.15}_{-0.18}$
Ω [rad]	2.20 ± 0.13	$0.335^{+0.087}_{-0.083}$	1.29 ± 0.25	$3.848^{+0.083}_{-0.089}$	$1.15^{+0.14}_{-0.11}$
ϖ [mas]	28.99 ± 0.020	29.01 ± 0.024	14.195 ± 0.016	28.20 ± 0.011	14.11 ± 0.019
ε (%)	$\equiv 0$	$\equiv 0$	$\equiv 0$	1.00 ± 0.12	$\equiv 0$

Notes. M is the primary mass; m is the secondary mass, P is the orbital period, $t_{\rm p}$ is the Julian date of pericenter minus 2,457,389.0, e is the eccentricity, $\cos I$ is the cosine of the inclination, ω is the argument of pericenter, Ω is the longitude of the ascending node, ϖ is the parallax, and ε is the flux ratio.
[a] Results for HIP 66074 should be interpreted cautiously because of the unrealistically high flux ratio.
[b] Results for HD 175167 should be interpreted cautiously because of the tension between the Doppler-only and Gaia-only orbital parameters.

planet around this star with the Doppler technique. They estimated the star's age to be 0.8 Gyr based on its chromospheric activity level and the detection of lithium in its spectrum. Li et al. (2021) used a different activity/age calibration to arrive at an age of 1.8 ± 0.3 Gyr, which is also consistent with the measured rotation period of 15–16 days. Li et al. (2021) also spearheaded the effort to combine Doppler and Gaia data for this star. Although they did not have the Gaia two-body solution at their disposal, they constrained the three-dimensional orbital configuration by combining the radial-velocity data with a measurement of the star's secular acceleration, which was in turn based on the difference between the Hipparcos and Gaia proper motions.

The radial-velocity data span three planetary orbits but because of spotty time coverage, the parameters of the Doppler-only fit were not constrained as well as they were for BD-17 0063. In particular, the posterior distribution for the period is bimodal, with a peak at the favored period at about 1000 days and a secondary peak at about 1100 days containing about one-third of the total probability.

Of the two periods, the 1000 day period agrees better with the period of the Gaia astrometric orbit (833 ± 110 days). The two periods are about 1.5σ apart. Likewise, the Doppler-only and Gaia-only values of the eccentricity agree to within 1.5σ, with $e = 0.530^{+0.048}_{-0.073}$ from the Doppler data and 0.35 ± 0.15 from the Gaia orbital solution. The time of pericenter, argument of pericenter, and K values agree to within 1σ.

Thus, a joint fit seemed warranted. The best-fit model was able to reproduce all of the relevant characteristics of the Doppler data and the Gaia orbital solution. The flux ratio was bounded to be below 0.098% with 95% confidence, another mark of consistency. For the final results, the joint fit was repeated under the constraint $\varepsilon = 0$. Figure 2 shows the fit in the same format as in Figure 1, and the corner plot can be found in the Appendix. The orbital period is 1004.7 ± 3.0 days, the planet's mass is 7.53 ± 0.32 Jupiter masses, and the orbital eccentricity is $0.527^{+0.034}_{-0.037}$. The inclination is $111.4^{+4.4}_{-4.7}$ deg.

The results of the joint fit are also compatible with those of Li et al. (2021), who found a planet mass of $7.24^{+1.0}_{-0.37}$ Jupiter masses and an eccentricity of 0.525 ± 0.025. Their results for the inclination were subject to a two-way discrete degeneracy, with $I = 73^{+12}_{-16}$ or 107^{+16}_{-12} deg, the latter of which agrees with the results presented here.

4.3. HD 132406

da Silva et al. (2007) reported a giant planet orbiting HD 132406 (BD+53 1752, HIP 73146), a G star at a distance of 70 pc with $G = 8.3$. They selected this star for their survey on account of its relatively high metallicity ($[{\rm Fe/H}] = +0.18 \pm 0.05$). The team was trying to exploit the strong association between metallicity and giant-planet occurrence in order to find as many giant planets as possible. They reported $m \sin I = 5.61\ M_{\rm Jup}$, $e = 0.34$, and $P = 974$ days. The literature has remained quiet about this star since 2007. For this study, a stellar mass of $0.973 \pm 0.040\ M_\odot$ was adopted, based on the FLAME results.

This was a case in which neither the Doppler data nor the Gaia data were very constraining by themselves. The Doppler data extend over only one orbital cycle, and the velocity extrema are poorly covered. The Doppler-only analysis gave $K = 117^{+179}_{-22}$ m s^{-1}. Likewise, Gaia detected the astrometric orbit with a relatively modest statistical significance ($a_0 = 0.172^{+0.058}_{-0.034}$ mas), leading to a predicted K value of 131^{+80}_{-53} m s^{-1}.

The Doppler and Gaia results for the K parameter and all of the other parameters they have in common were found to be in agreement, justifying a joint fit. This pinned down the K value to 101 ± 10 m s^{-1}. However, the Gaia data cannot strongly exclude a nearly face-on orbit; in the joint fit, the cosine of the inclination is -0.81 ± 0.14. As a result, the posterior probability distribution for the companion mass has a long tail extending to high values. The marginalized result is $m = 7.9^{+6.8}_{-1.6}$ Jupiter masses, extending into the brown-dwarf regime. Higher companion masses are associated with higher flux ratios, following the approximate relation $\varepsilon \approx 0.9 \times 10^{-3}\, m/M_{\rm Jup}$. Essentially, the orbit can be nudged closer to face on if the companion mass is increased (to keep $m \sin I$ constant and maintain agreement with the Doppler data) and the flux ratio is increased (to preserve the size of the observed orbit and maintain agreement with the Gaia data).

To prevent the results from being influenced by statistically acceptable models with unrealistically high flux ratios, the fit was repeated under the constraint $\varepsilon = 0$. This broke the m/I degeneracy, leading to the results $m = 5.94^{+0.65}_{-0.59}\ M_{\rm Jup}$ and $\cos I = -0.636^{+0.113}_{-0.086}$. The orbit is mildly eccentric, with

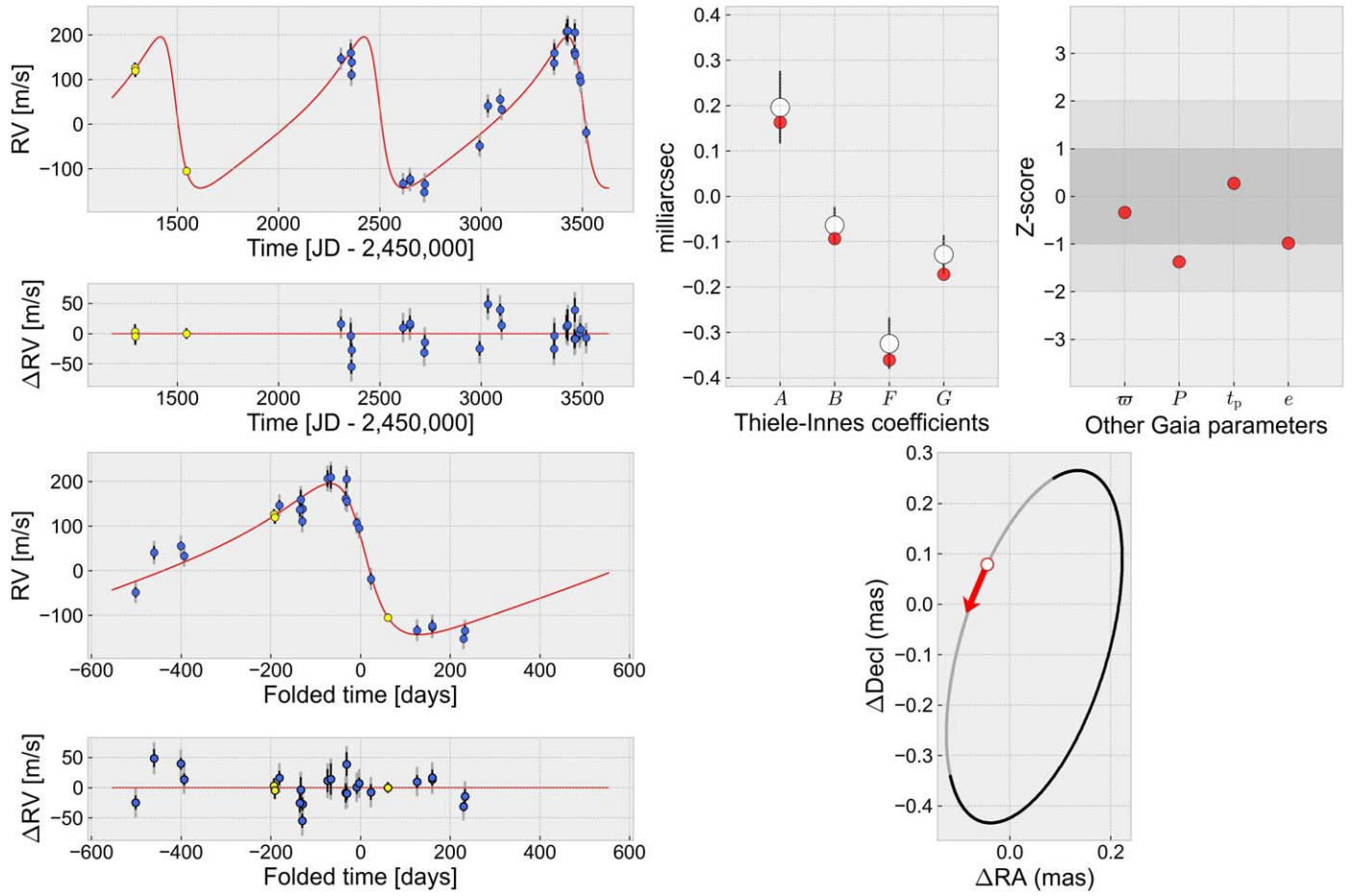

Figure 2. HD 81040: results of the joint Gaia–Doppler fit, assuming the companion is dark. Same format as Figure 1. In the radial-velocity plots, the filled symbols are from ELODIE and the open symbols are from HIRES.

$e = 0.250^{+0.063}_{-0.075}$. The results are given in Table 2 and depicted in Figure 3. A corner plot can be found in the Appendix.

4.4. HIP 66074

HIP 66704 (BD+75 510, GJ 9452) is a K dwarf at a distance of 35 pc with a Gaia optical magnitude of $G = 9.7$. The `gaiadr3.astrophysical_parameters` table does not provide a mass estimate, but does provide a spectroscopy-based effective temperature of 4161 ± 3 K (`teff_gspspec`). The absolute G magnitude implied by the apparent magnitude and parallax is 7.0. A mass of $0.67 \pm 0.05\ M_\odot$ was adopted for this star, based on the effective temperature, the absolute magnitude, and the online version of Table 5 of Pecaut & Mamajek (2013).

The star was monitored in the Lick-Carnegie Exoplanet Survey, although no planet had been announced prior to Gaia DR3. The 10 available radial velocities were taken from the catalog of Butler et al. (2017).[5] The Gaia team reported that the star shows astrometric motion consistent with the presence of a giant planet with a mass of $7.3\ M_{\rm Jup}$ and $P = 297$ days (Gaia Collaboration et al. 2022b; Holl et al. 2022).

For the Doppler-only analysis, a good fit was found with $P = 301 \pm 5$ days, $K = 19^{+14}_{-3}$ m s^{-1}, $t_{\rm p} = 62^{+37}_{-32}$ days, $e = 0.45 \pm 0.22$, and $\omega = 261^{+23}_{-30}$ deg. As is typical with meager Doppler data sets, the joint posterior probability distribution includes a long tail encompassing models with high K and high e that produce "velocity spikes" during time ranges when no data were obtained.

According to the Gaia two-body orbital solution, $P = 297.9 \pm 2.7$ days, $e = 0.40 \pm 0.17$, $t_{\rm p} = 58 \pm 26$ days, and $\omega = 265° \pm 19°$. All of these parameters are within 1σ of the corresponding Doppler-only parameters. However, there is a serious problem with the radial-velocity semiamplitude. The Gaia-only value is $K = 297^{+82}_{-62}$ m s^{-1}, 15 times (4.4σ) higher than the Doppler-only value.

Because of this problem, it is unclear whether a joint fit is justified, although it was performed anyways. In fact, an excellent fit was achieved to all of the data (see Figure 4). The sole peculiarity is that the flux ratio is 0.0100 ± 0.0012, i.e., incompatible with zero. The effect of the nonzero flux ratio is to cause the motion of the center of light—the motion that is tracked by Gaia—to be reduced relative to the motion of the primary star. This allows the orbit of the primary star to be wider and the orbital speed to be slower, thereby reconciling the Gaia orbital solution with the low K value implied by the Doppler data.

A flux ratio on the order of 10^{-2} does not seem realistic, though, given that the mass ratio was found to be $(6.3^{+0.7}_{-0.6}) \times 10^{-4}$. No reasonable mass/luminosity relationship for brown dwarfs or planets would predict an optical flux ratio

[5] The catalog includes an 11th data point based on a spectrum with a much lower signal-to-noise ratio than the others, which was not used here. The time stamp of the omitted point is 2455042.76395.

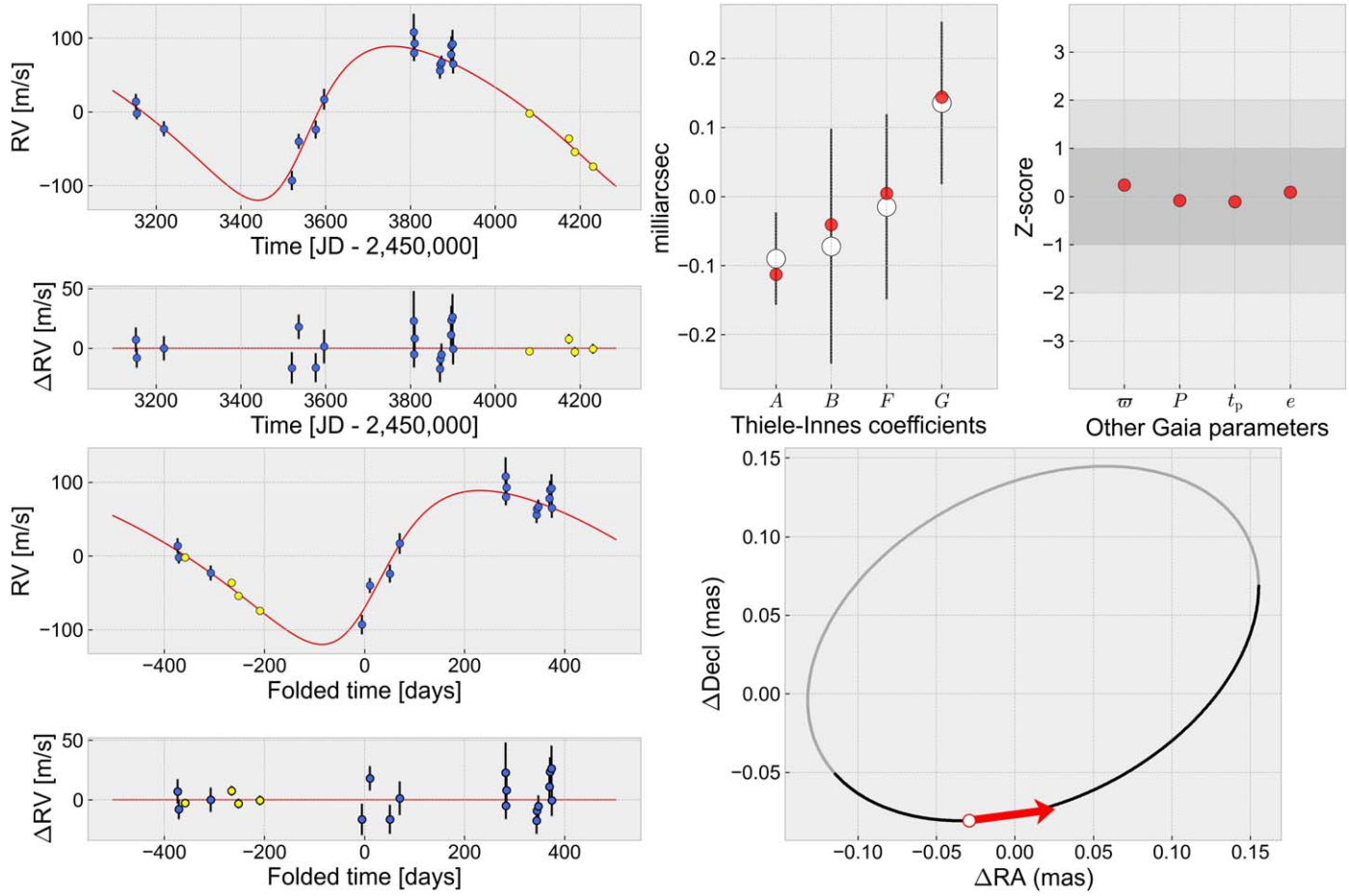

Figure 3. HD 132406: results of jointly fitting the Doppler data and Gaia two-body orbital solution, assuming the companion is dark. Same format as Figure 1. In the radial-velocity plots, the filled symbols are from ELODIE, and the open symbols are from SOPHIE.

that is more than an order of magnitude higher than the mass ratio.

Another way to state the problem is as follows. The Doppler data require that $m \sin I = 0.435^{+0.038}_{-0.078}$ Jupiter masses, and the Gaia two-body solution involves a high inclination ($I = 91 \pm 5$ deg), thereby cementing the companion's mass within the planetary-mass regime and leading to a strong presumption that the flux ratio is $\ll 10^{-4}$. However, the semimajor axis of the astrometric orbit measured by Gaia is too large to be compatible with a dark planetary-mass object. The tension is at the 10σ level.

The reason for the discrepancy is unclear. Perhaps the system is home to more than just a single companion, and the results of Doppler analysis, the Gaia two-body solution, or both, were thrown off by the unmodeled effects of additional bodies. Unfortunately, there are not enough Doppler data, and not enough information in Gaia DR3, to consider this hypothesis in detail. Obtaining more Doppler data would help to clarify the situation.

4.5. HD 175167

HD 175167 (HIP 93281) is a metal-rich G star ([Fe/H] = +0.19) located 71 pc away, with $G = 7.8$ and a FLAME-based mass of $1.09 \pm 0.04\,M_\odot$. Arriagada et al. (2010) used the Doppler technique to identify a giant planet with $K = 161$ m s^{-1}, $P = 1290$ days, and $e = 0.54$, which together give $m \sin I = 7.8$ Jupiter masses. Only 13 velocities are available, and there are no other accounts of precise Doppler observations in the literature.

The available Doppler data span only 1.4 orbital periods, leading to a strong covariance between the uncertainties of P and t_p. The posterior probability distribution for the orbital period is highly skewed. Marginalizing over t_p and all other parameters, the Doppler-only estimate for the orbital period is 1283^{+14}_{-42} days. The posterior for the orbital eccentricity is skewed, too, giving $e = 0.536^{+0.149}_{-0.035}$. As was the case with HIP 66074, the Doppler-only fit admits the possibility of high-e solutions with huge velocity excursions when nobody was looking.

The Gaia DR3 orbital parameters are subject to unusually large uncertainties, probably because the time span of the Gaia observations (1038 days) is shorter than the planet's orbital period. According to the Gaia two-body orbital solution, $P = 899 \pm 198$ days and $e = 0.19 \pm 0.12$. The Gaia period is about 2σ lower than the Doppler-only period, and the Gaia eccentricity is about 3σ lower than the Doppler-only eccentricity, although such "number-of-sigma" comparisons are often misleading when the uncertainty distributions are non-Gaussian. The stated uncertainty in the time of periastron, 737 days, is comparable to the period itself. Given that the uncertainties in the Gaia orbital parameters are large and probably non-Gaussian, this may be a case in which the tabulated best-fit values and correlation matrix elements do not

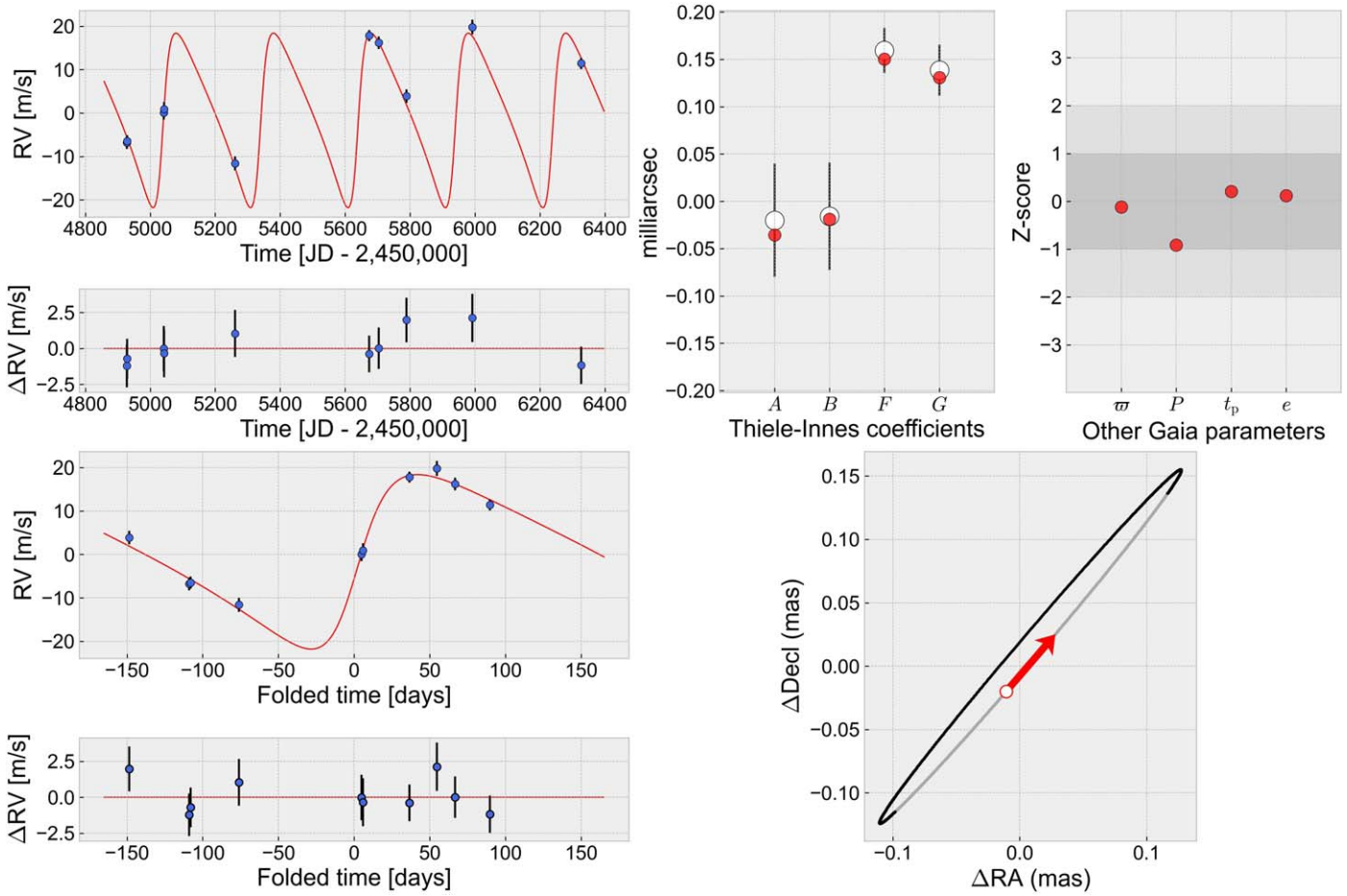

Figure 4. HIP 66074: results of jointly fitting the Doppler data and Gaia two-body orbital solution. Same format as Figure 1.

provide enough information for an accurate treatment of the uncertainties.

With this caveat in mind, a joint fit was undertaken. The model was able to provide a good fit to the RV data and was also successful in reproducing the measured Thiele–Innes coefficients. The joint-fit eccentricity is about 2.5σ higher than the Gaia-only value, a sign of unrelieved stress between the Doppler data and the Gaia orbital solution. The joint fit gives a companion mass of $18.1^{+5.5}_{-2.9}$ Jupiter masses, suggesting that the companion might be better designated as a brown dwarf than a giant planet. The flux ratio converged on small values, with a 95% confidence upper bound of 1.5%.

As was the case for HD 132406, the allowed region in parameter space includes a thin "branch" of solutions with very low inclinations, relatively high companion masses, and unrealistically high flux ratios ($\sim$1%). To suppress this solution branch, the joint fit was repeated under the constraint $\varepsilon = 0$. The companion's mass was thereby pinned down to be $14.8^{+1.8}_{-1.6}$ Jupiter masses, with a corresponding orbital inclination of $35.5° \pm 2.3°$. The results are given in Table 2, Figure 5, and the Appendix. They should be interpreted cautiously because of the large and non-Gaussian uncertainties in the Gaia orbital solution.

4.6. HR 810

HR 810 (Iota Horologium, HD 17051; HIP 12653 GJ 108) is a G0 star 17 pc away that shows X-ray and Ca II emission characteristic of young stars. Kürster et al. (2000) reported that the star is on the zero-age main sequence, with an age between 30 Myr and 2 Gyr. Long-term monitoring of its ultraviolet flux, X-ray flux, and chromospheric emission lines has given evidence for stellar activity cycles with durations of a few years (see, e.g., Flores et al. 2017; Sanz-Forcada et al. 2019). The star's mass is 1.077 ± 0.040 according to the Gaia DR3 FLAME code. With a Gaia optical magnitude of $G = 5.3$, HR 810 is brighter than the other stars analyzed in this work.

A giant planet orbiting HR 810 with a minimum mass of $2.2\,M_{\rm Jup}$ and a period of 320 days was discovered by Kürster et al. (2000) using the Doppler technique and confirmed with additional data from Butler et al. (2001) and Naef et al. (2001). Additional Doppler data are also available in the user-friendly HARPS archive created by Trifonov et al. (2020).

According to the Doppler-only analysis, the radial-velocity semiamplitude and orbital period are well constrained, with $K = 61.1 \pm 2.5$ m s^{-1} and $P = 308.8 \pm 0.6$ days. The orbit is nearly circular, with $e = 0.105^{+0.040}_{-0.046}$. However, as is typical of young and chromospherically active stars, the Doppler data appear to be affected by systematic errors in excess of the formal measurement precision. The model responds by enlarging the "jitter" parameters as needed, but the accuracy of the results hinges on the assumption implicit in Equation (4) that the errors are independently drawn from a time-invariant Gaussian distribution. In this case, the residuals are correlated in time, as can be seen in Figure 6. In addition to the large scatter observed in the residuals, there are hints of a 1400 day periodicity, with maxima at time coordinates 200, 1600, and

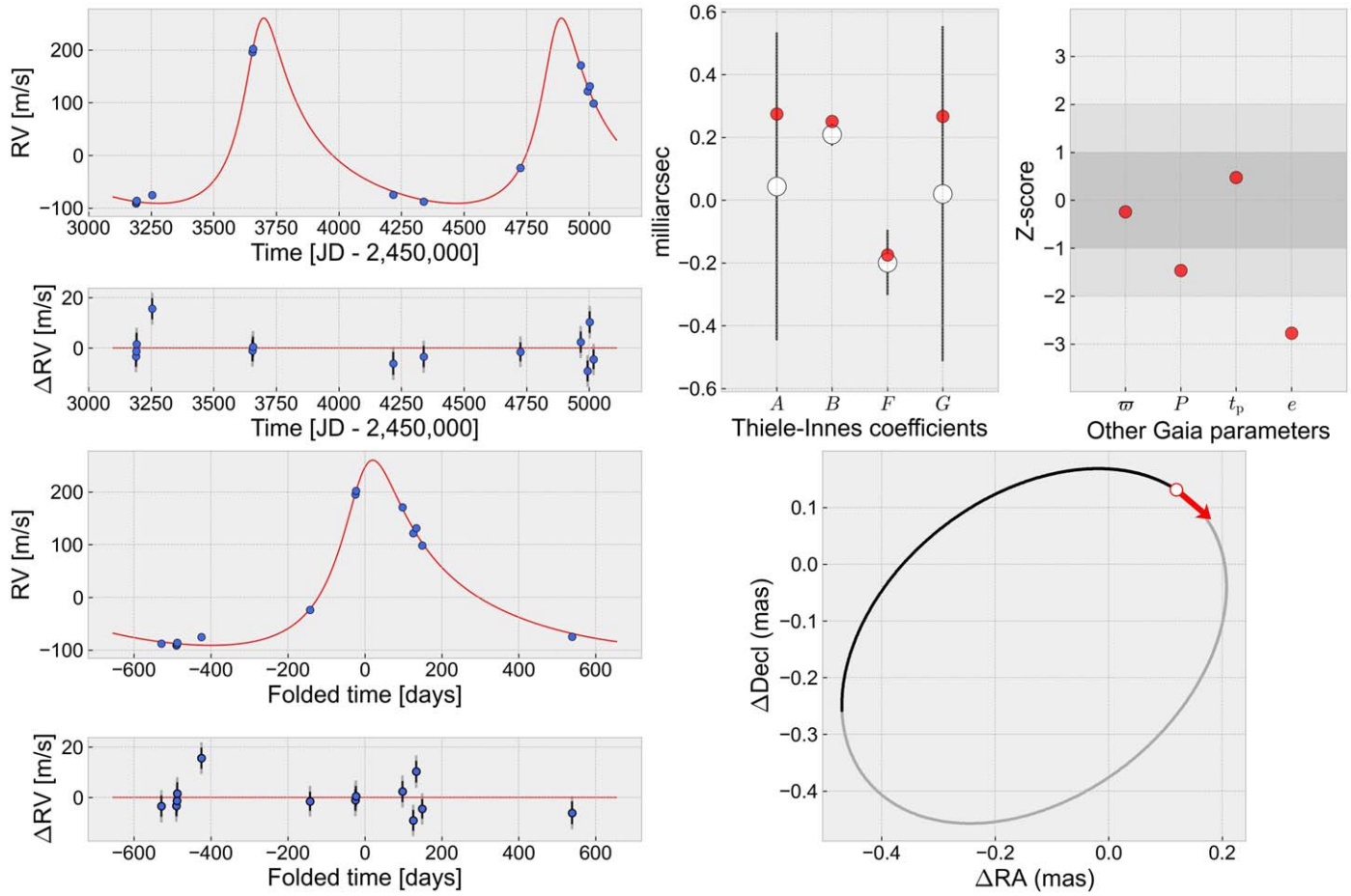

Figure 5. HD 175167: results of jointly fitting the Doppler and astrometric data. Same format as Figure 1.

3000. These undulations could be due to an additional planet or stellar activity.

For HR 810, the tabulated "astrometric jitter" parameter (which plays the same role in the astrometric fit as the "velocity jitter" does in the Doppler fit) is 0.279 mas, about three times larger than for any of the other stars analyzed in this work. However, by itself, the relatively high jitter is not necessarily a symptom of a problem with the Gaia two-body solution. Jitter values between 0.2 and 0.5 mas are typical for stars as bright as HR 810, which exceed the nominal Gaia bright limit of $G = 5.7$ (see Figure A.1 of Lindegren et al. 2021).

More worrying is that the tabulated Gaia orbital elements for this star are highly uncertain. All of the Thiele–Innes coefficients are compatible with zero to within the formal uncertainties. This fact may be related to an issue that was described by Gaia Collaboration et al. (2022b): When the eccentricity is low, the two-body fitting code tends to overestimate the uncertainties in the Thiele–Innes coefficients. This issue led Babusiaux et al. (2022) to warn that "the covariance matrix for very low eccentricity solutions may be problematic." Thus, this is probably another case in which knowledge of the tabulated best-fit values and correlation matrix is insufficient for an accurate treatment of the uncertainties.

The Gaia-only period is 333.0 ± 5.8 days, which is close enough to the Doppler-only period that it is unlikely to be a coincidence. However, the two periods disagree by 4σ. The Gaia-only prediction for K is 205^{+102}_{-31} m s^{-1}, another 4σ discrepancy with the Doppler-only analysis. The Gaia-only eccentricity is $0.14^{+0.15}_{-0.10}$, which does agree with the Doppler-only analysis.

Given the reasons to be skeptical of both the Doppler and the Gaia analyses, the quantitative results of the joint fit must be taken with a grain of salt. Indeed, in the joint fit, the compromise that was struck between the Doppler data and the Gaia orbital solution seems unsatisfactory. The orbit was found to be nearly face on ($\cos I = 0.957^{+0.037}_{-0.069}$, or $I = 17 \pm 10$ deg), even though the Gaia-only fit prefers an edge-on orbit ($\cos I = 0.050 \pm 0.085$). The joint solution exhibits the same strong degeneracy between m, I, and ε that was seen for HD 132406 (Section 4.3).

Because of the patterned residuals in the Doppler data, the large formal uncertainties in the Gaia two-body solution, and the statistical disagreement between the Doppler-only and Gaia-only analyses, the quantitative results for the joint fit are not given in Table 2, although they are depicted in Figure 6 and in the Appendix.

4.7. HD 111232

HD 111232 (HIP 62534) is a G star located 29 pc away with a Gaia optical magnitude of $G = 7.4$. Its mass is $0.897 \pm 0.04\,M_\odot$, based on the FLAME parameters tabulated in Gaia DR3. Mayor et al. (2004) discovered a giant planet around this star, as part of a survey with the CORALIE spectrograph. The star is relatively metal deficient, with [Fe/H] = −0.36. Based on the low metallicity

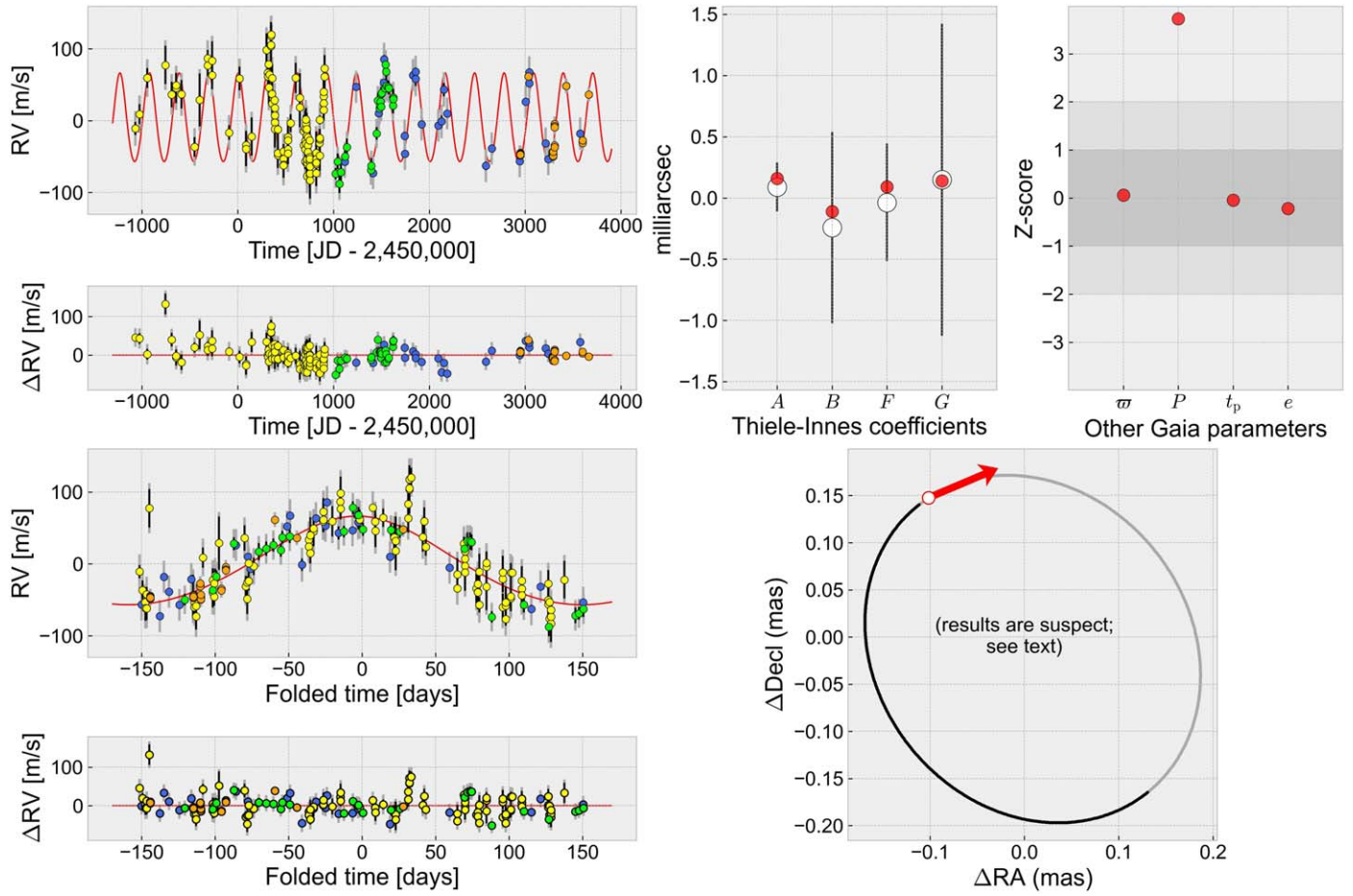

Figure 6. HR 810: results of jointly fitting the Doppler and astrometric data. Same format as Figure 1. The results should be viewed skeptically; see the text for details.

as well as a high space velocity of 104.4 km s^{-1}, Mayor et al. (2004) proposed that the star belongs to the galaxy's "thick disk." Their best-fit Doppler orbit had $P = 1118$ days, $e = 0.19$, and $m \sin I = 6.7$ Jupiter masses.

The star was also observed by Minniti et al. (2009) with the MIKE spectrograph as part of the Magellan Planet Search Program. Their independent data set provided strong confirmatory evidence for the planet. However, they did not fit the CORALIE and MIKE data simultaneously. Had they done so, they would have found that the combined data set is incompatible with a single-planet solution. Additional data from the HARPS public archive prepared by Trifonov et al. (2020) confirm this conclusion. Figure 7 shows all of the radial-velocity data.

The red curve is the best-fitting model involving a single planet and an ad hoc quadratic function of time. The model provides a decent qualitative description of most of the data, but the residuals show clear patterns and major outliers. In this model, $P = 917$ days, which is closer to the Gaia-derived value of 882 ± 30 days than the originally reported periods of 1118 days (Minniti et al. 2009) and 1143 days (Mayor et al. 2004). The model's eccentricity of 0.081 is inconsistent with the Gaia-derived eccentricity of 0.5 ± 0.1.

Clearly, there is more to this system than a star and a single giant planet. A joint fit was not performed because the results of such a fit would be incoherent. The star's additional motion is obvious in the Doppler data and could also have affected the astrometric measurements over the ≈1000 day time span of the Gaia observations.

4.8. HD 114762

HD 114762 (BD+18 2700, HIP 64426) is an early-G or late-F star at a distance of 39 pc, with $G = 7.1$. There are discrepant reports of its effective temperature: 5673 ± 44 K (Kane et al. 2011), 5730^{+37}_{-130} K (`gspspec_teff`), 5837 ± 31 K (Ghezzi et al. 2010), 5869 ± 13 K (Stassun et al. 2017), and 5935 ± 1 K (`gspphot_teff`). Perhaps the differences are related to the star's low metallicity (-0.77 ± 0.03, per Kane et al. 2011, or -0.66 ± 0.02, per Sousa et al. 2021). The Gaia DR3 FLAME mass, $1.047 \pm 0.040\, M_\odot$, is adopted here.

HD 114762 played an important role in the history of exoplanetary science. Latham et al. (1989) found radial-velocity variations with a period of 84 days, an eccentricity of 0.3, and an implied $m \sin I$ of 11 Jupiter masses. The authors wrote that the companion was "a good candidate to be a brown dwarf or even a giant planet." Either discovery would have been the first of its kind.

The prolonged debate over whether the companion was likely to be an exoplanet took some interesting turns. Initially, it was unclear whether a giant planet could have such a high mass, high eccentricity, and short period. Of course, we now know of many giant planets with high eccentricities and short periods, and there are many objects with masses of 10–20

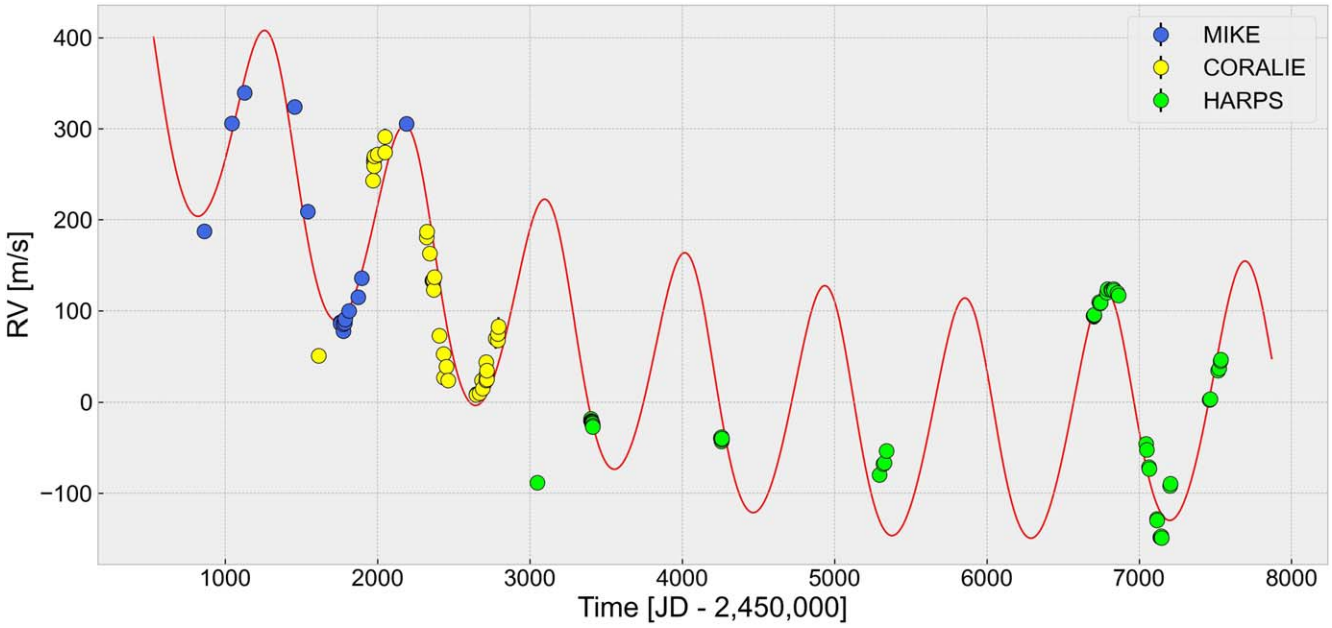

Figure 7. HD 111232: Doppler data and the best-fit model, including a single planet and an ad hoc quadratic function of time representing the effects of other bodies.

Jupiter masses that are classified as exoplanets in the NASA Exoplanet Archive.

By the early 2000s, the occurrence of short-period giant planets was known to be strongly associated with high metallicity (Santos et al. 2001; Fischer & Valenti 2005). This allowed another argument to be lodged against planethood for the companion of the metal-poor star HD 114762.

In addition, there was the generic problem common to all Doppler planets: The unknown inclination angle leaves open the possibility that the orbit is being viewed at low inclination, and m is much larger than $m \sin I$. In an attempt to constrain the inclination, Cochran et al. (1991) placed an upper bound of 1 km s^{-1} on the star's projected rotation velocity, which is anomalously low for stars of the same spectral type. This suggested that the star's rotation axis has a low inclination and —if the orbit is aligned with the star—the orbit is viewed nearly face on. The premise of good alignment was reasonable at the time but was eventually undermined by the discovery of severe misalignments between stars and the orbits of short-period giant planets (see Albrecht et al. 2022 for a review).

Kiefer (2019) overcame the impasse using information from Gaia's first data release. Although this data release did not include time-series astrometry, nor the results of two-body fits, it did report the "astrometric excess noise," a measure of goodness of fit to a model in which the star has no companions. After performing simulations of possible orbits and the corresponding levels of astrometric excess noise that they would produce, Kiefer (2019) concluded that HD 114762's orbital inclination is only 4°–6° and the secondary mass is $0.13 \pm 0.03\,M_{\odot}$. Later, using DR3 data, Gaia Collaboration et al. (2022b) and Holl et al. (2022) confirmed that HD 114762 is a face-on binary star.

Although the saga of HD 114762b as a planet candidate has ended, a joint analysis of all the available data was performed for the sake of completeness. For this case, a minor change was made to the fitting procedure: The parameters $\omega + \Omega$ and $\omega - \Omega$ were used in the MCMC analysis rather than ω and Ω. This is because, for nearly face-on binaries, $\omega + \Omega$ can be measured precisely even though ω and Ω are degenerate.

Given the large quantity of Doppler data spanning more than 30 yr, the parameters of the spectroscopic orbit are rigidly nailed down. The Doppler-only analysis gave $P = 83.91713 \pm 0.00064$ days, $K = 620.1 \pm 0.85$ m s^{-1}, and $e = 0.3442 \pm 0.0012$. These and the other Doppler parameters were found to be consistent with the Gaia DR3 two-body orbital solution. The joint fit does not exhibit any significant tension. The orbital inclination is $2.8° \pm 0.6°$, and the secondary mass is $0.293^{+0.103}_{-0.056}\,M_{\odot}$. One would expect a binary star to have a nonzero flux ratio, and indeed, the flux ratio was found to be $0.052^{+0.070}_{-0.039}$.

Strong covariances exist between the uncertainties of the secondary mass, the orbital inclination, and the flux ratio, for the same reason that they were observed for HD 132406 (Section 4.3). To break this degeneracy, a simple mass–luminosity relationship was employed. The online version of Table 5 of Pecaut & Mamajek (2013) gives the absolute G magnitude as a function of stellar mass. For masses between 0.15 and 1.1 $M_{\odot}$, the results are well described by a quadratic function,

$$M_G = c_0 + c_1 m + c_2 m^2, \tag{18}$$

where m is the stellar mass (in solar masses) and the best-fit coefficients are $c_0 = 14.14$, $c_1 = -12.191$, and $c_2 = 2.713$.

The joint fit was repeated, this time with a Gaussian prior on the magnitude difference between the two stars with a mean determined by the application of Equation (18) to both stars, and a standard deviation of 0.25 (chosen somewhat arbitrarily). The prior constraint on the primary star's mass was also loosened from 1.047 ± 0.040 to 1.05 ± 0.10 solar masses to allow for the possibility that light from the companion affected the classification of the primary star. The effect of these changes was to suppress the solutions with relatively high flux ratios. The inclination, secondary mass, and flux ratio found through this procedure were $3.63° \pm 0.06°$, $0.215 \pm 0.013\,M_{\odot}$,

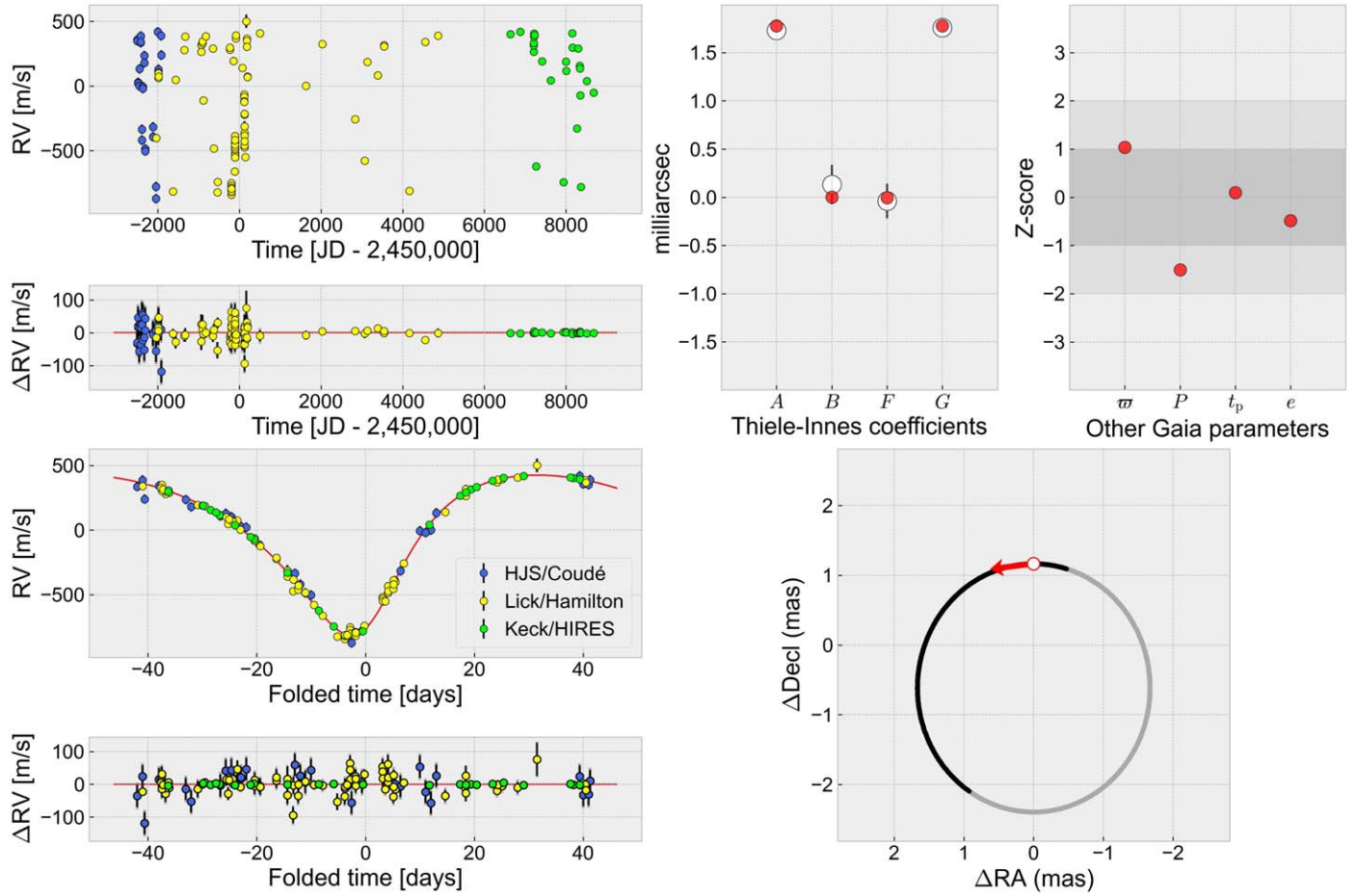

Figure 8. HD 114762: results of jointly fitting the Doppler and astrometric data. Same format as Figure 1, except that the model curve is not shown in the upper-left panel because the plotted time range spans too many cycles for the details to be visible. In the radial-velocity plots, the blue, yellow, and green points are from the Coude spectrograph on the Harlan J. Smith telescope (Cochran et al. 1991), the Lick/Hamilton spectrograph (Kane et al. 2011), and Keck/HIRES (Rosenthal et al. 2021), respectively.

Table 3
Results of Jointly Fitting the Doppler and Gaia Orbital Solution for HD 114762

Parameter # of	Value (no M/L prior)	Value (with M/L prior)
M [$M_\odot$]	1.046 ± 0.040	1.00 ± 0.10
m [$M_\odot$]	$0.293^{+0.103}_{-0.056}$	0.215 ± 0.013
P [days]	83.91712 ± 0.00064	83.91712 ± 0.00064
t_p [days]	-30.798 ± 0.048	-30.795 ± 0.048
e	0.3442 ± 0.0012	0.3442 ± 0.0012
$\cos I$	$0.99877^{+0.00049}_{-0.00054}$	0.997994 ± 0.000067
$\omega + \Omega$ [rad]	6.283 ± 0.013	6.283 ± 0.013
$\omega - \Omega$ [rad]	0.830 ± 0.014	0.831 ± 0.014
ϖ [mas]	25.35 ± 0.035	25.35 ± 0.035
ε [%]	$5.2^{+7.1}_{-3.9}$	$0.17^{+0.14}_{-0.07}$

Note. The M/L prior refers to a prior constraint on the relationship between the mass ratio and the flux ratio in the Gaia G band. See Equation (18).

and $0.17^{+0.14}_{-0.07}$%, respectively. The results are given in Table 3 and depicted in Figure 8, with the corner plot in the Appendix.

In this model, $\cos I = 0.997994 \pm 0.000067$, remarkably close to unity. Only one out of ≈500 binaries in a randomly oriented sample would be expected to have such a low inclination. Of course, HD 114762 was not drawn at random from such a sample. It drew attention because of the low amplitude of the Doppler signal, a selection criterion favoring face-on orbits.

5. Discussion

Exoplanetary systems that can be studied with more than one technique are especially valuable. The data from different techniques can validate and reinforce each other, while also providing more powerful constraints on the system's parameters. At the moment, the most common combination is the pairing of the Doppler and transit techniques. The Doppler technique supplies $m \sin I$, and the transit technique ensures $I \approx 90°$ while also giving access to the planet's radius. According to the NASA Exoplanet Archive, there are 838 "confirmed" planets that have been detected by both the Doppler and transit techniques. The next most common combination is that of the Doppler and astrometric techniques. Until very recently, almost all such systems were Doppler planets for which astrometric motion was detected with the Hubble Space Telescope Fine Guidance Sensors (see, e.g., Benedict et al. 2002; McArthur et al. 2010), or through the comparison of Hipparcos and Gaia positions and proper motions (Li et al. 2021). Prior to Gaia DR3, there were about 15 objects in this category, with the exact number depending on the upper mass limit chosen for planets. A few directly

imaged planets have also been detected with the Doppler method (see, e.g., Ruffio et al. 2021).

Now, astrometric information is available for 73 planets and candidate planets, of which 9 were already known to exist from Doppler surveys. Simulations of the Gaia survey suggest that $\sim 10^4$ planets will eventually be detectable with Gaia data Perryman et al. (2014). Precise Doppler observations will play an important role in the validation and characterization of the planets with bright host stars, as emphasized by Gaia Collaboration et al. (2022b) and Holl et al. (2022), and as demonstrated in this study.

For now, the publicly available Gaia information is limited to the results of fitting a two-body model to the data, rather than the time-series astrometry. When the Gaia orbital parameters have nearly Gaussian uncertainties and the star's reflex motion is dominated by the effect of a single giant planet, there is no obstacle to combining the Doppler and Gaia information and obtaining good constraints on the three-dimensional orbit as well as the planet's mass, as was the case for BD-17 0063, HD 81040, and HD 132406. In some cases, though, the interpretation of the data will be more difficult because of non-Gaussian uncertainties, as was the case for HD 175167 and HR 810, or the presence of multiple planetary signals, as is the case for HD 111232 and possibly for HIP 66074.

Progress is possible now, but much will have to wait until Gaia DR4 when the time-series astrometric data will become available. In the meantime, it would be useful to conduct long-term Doppler monitoring of stars known to have giant planets that are potentially detectable with Gaia. Too many giant planets have been discovered with the Doppler method and then ignored for a decade or more. Obtaining at least a little more Doppler data over timescales of a few years before DR4 would enhance our ability to interpret the Gaia data and make the most of the enormous exoplanet potential of the Gaia mission.

This work would not have been possible without the hard work over many years of the Gaia team, who have delivered a data set with a breathtaking scope of applications. The author is also grateful to the anonymous referee for a timely and helpful report, and to D. Foreman-Mackey for his development of the `emcee` and `corner` Python codes. This work has made use of data from the European Space Agency (ESA) mission Gaia (https://www.cosmos.esa.int/gaia), processed by the Gaia Data Processing and Analysis Consortium (DPAC, https://www.cosmos.esa.int/web/gaia/dpac/consortium). Funding for the DPAC has been provided by national institutions, in particular the institutions participating in the Gaia Multilateral Agreement. This research also made use of the NASA Exoplanet Archive (2019), which is operated by the California Institute of Technology, under contract with the National Aeronautics and Space Administration under the Exoplanet Exploration Program.

Appendix
Corner plots

Contained here are plots of the joint a posteriori probability distribution of the parameters for each system, based on the simultaneous fit to the Doppler data and Gaia orbital solution, and depicted as a "corner plot" of 2D distributions. The results for BD-17 0063, HD 81040, HD 132406, HIP 66074, HD 175167, HR 810, and HD 114762 are shown in Figures 9, 10, 11, 12, 13, 14, and 15, respectively.

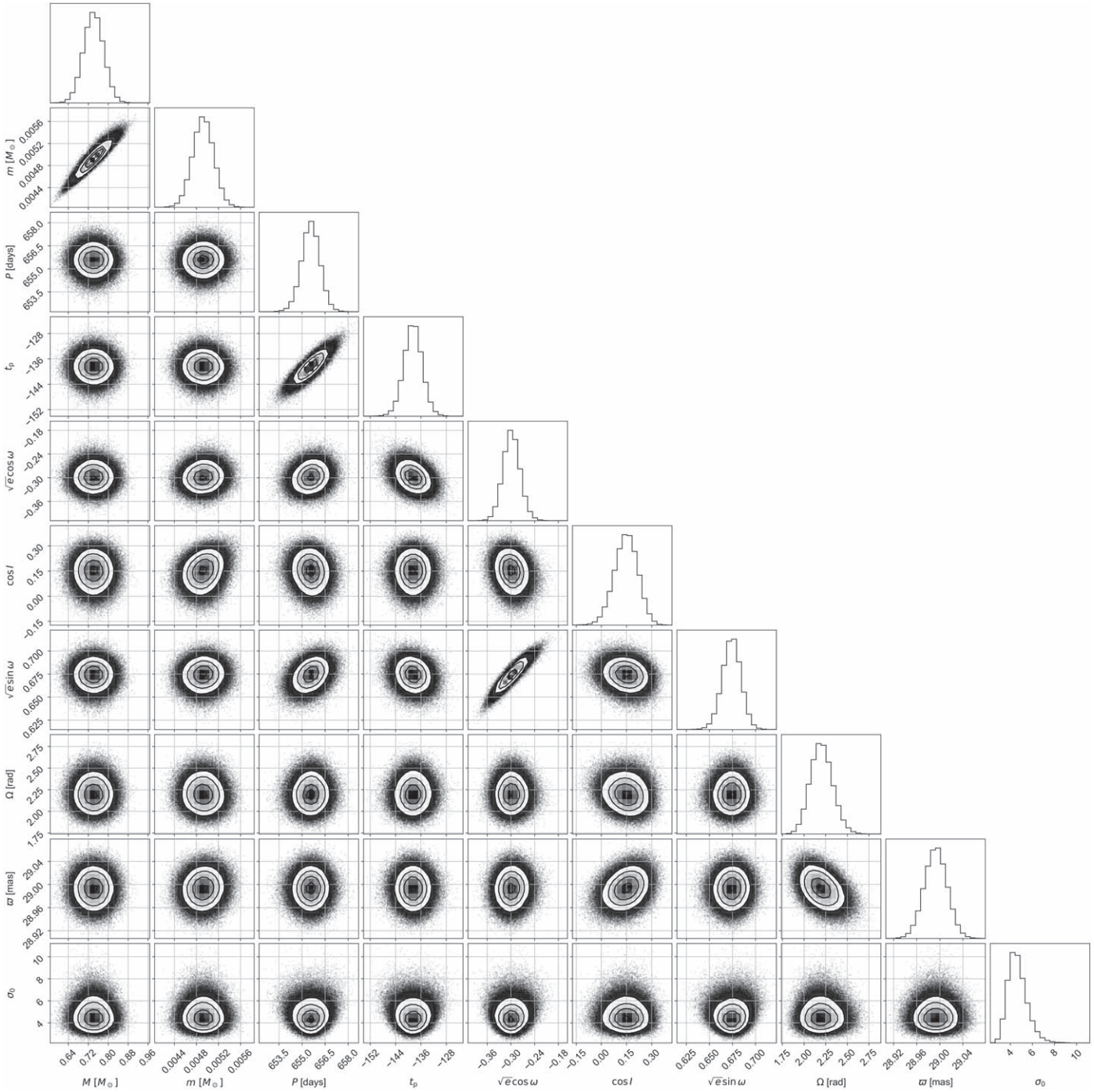

Figure 9. BD-17 0063.

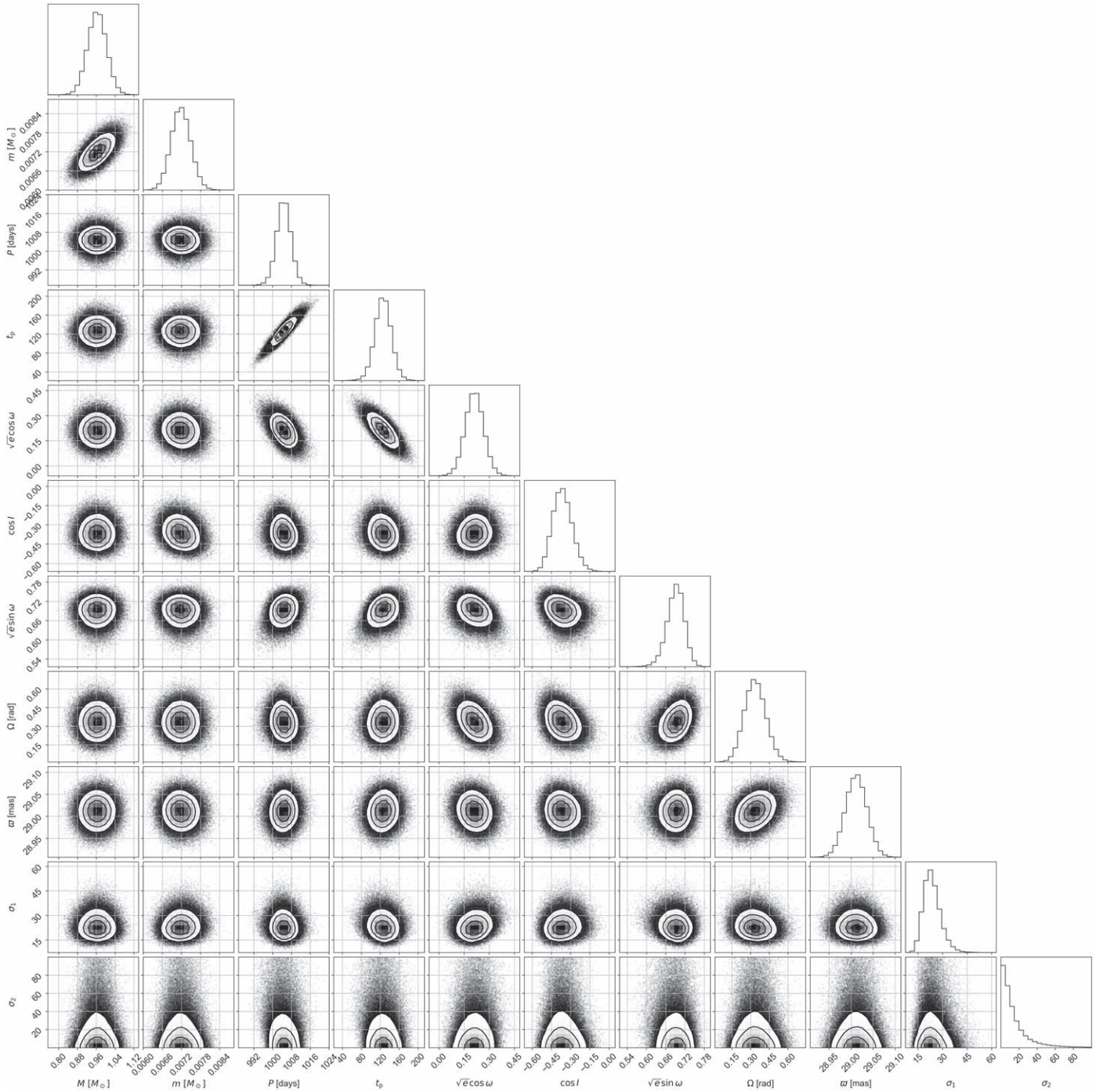

Figure 10. HD 81040.

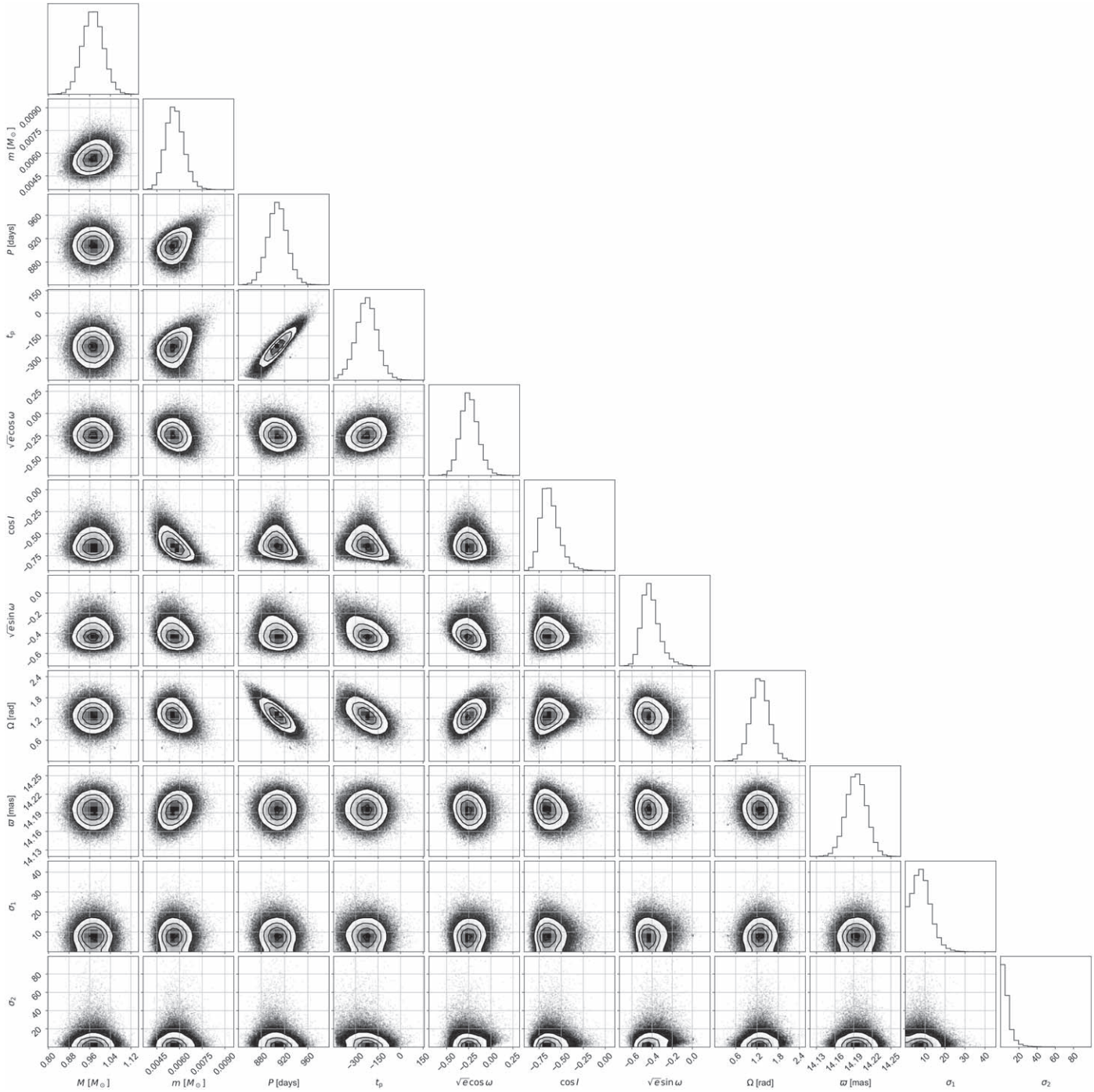

Figure 11. HD 132406.

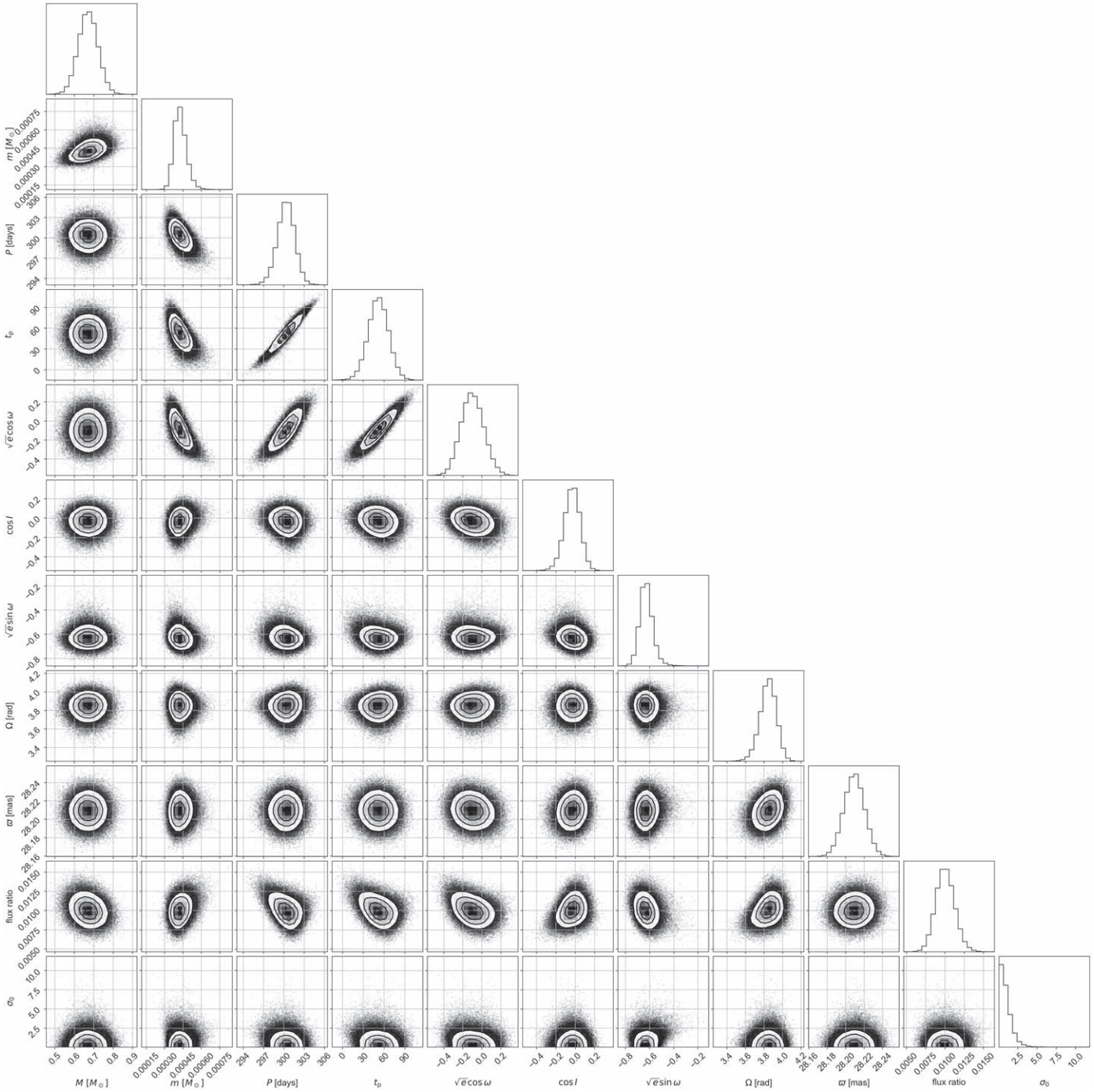

Figure 12. HIP 66074.

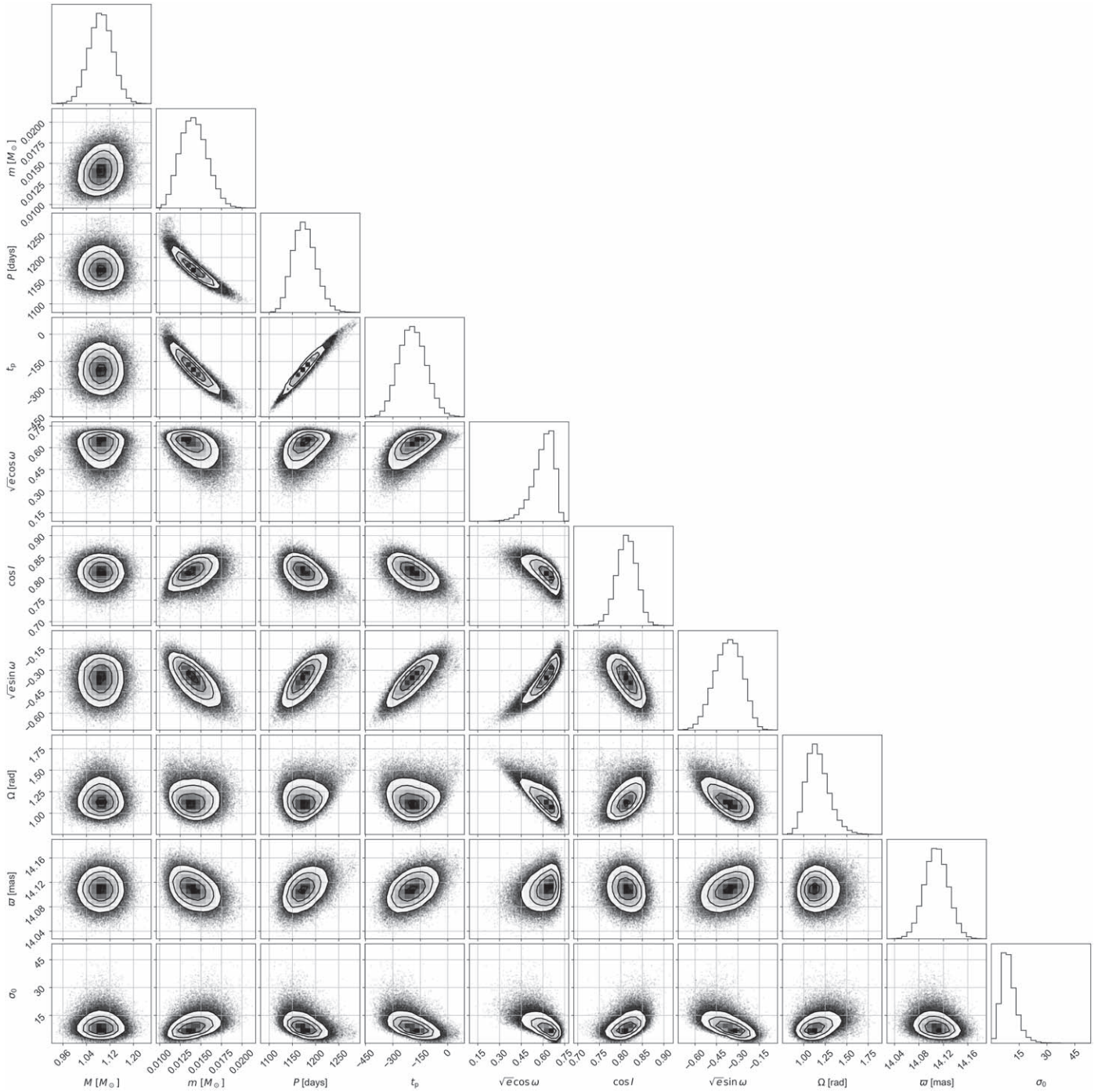

Figure 13. HD 175167.

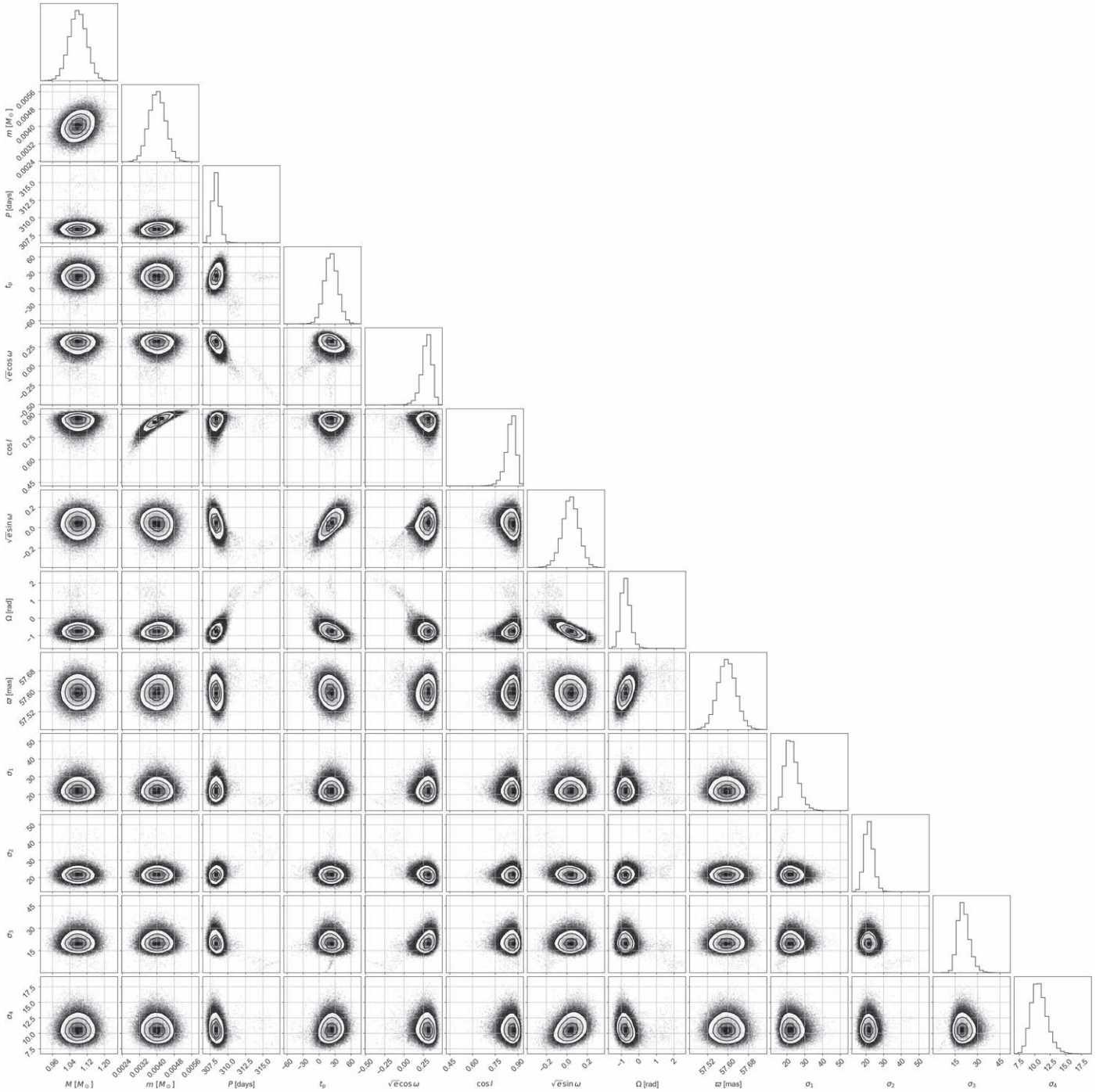

Figure 14. HR 810.

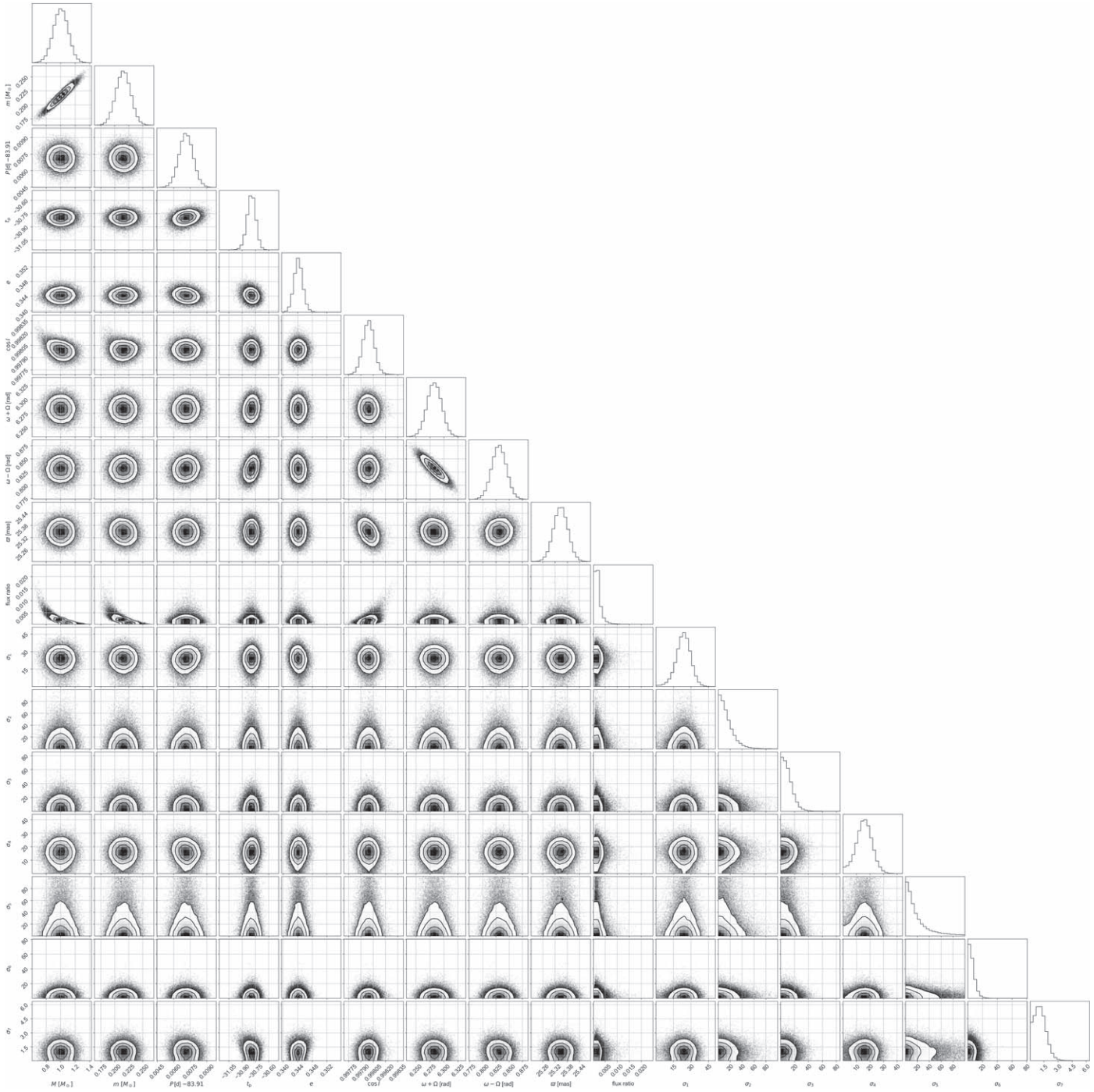

Figure 15. HD 114762.

ORCID iDs

Joshua N. Winn https://orcid.org/0000-0002-4265-047X

References

Albrecht, S. H., Dawson, R. I., & Winn, J. N. 2022, PASP, 134, 082001
Arriagada, P., Butler, R. P., Minniti, D., et al. 2010, ApJ, 711, 1229
Babusiaux, C., Fabricius, C., Khanna, S., et al. 2022, arXiv:2206.05989
Benedict, G. F., McArthur, B. E., Forveille, T., et al. 2002, ApJL, 581, L115
Butler, R. P., Tinney, C. G., Marcy, G. W., et al. 2001, ApJ, 555, 410
Butler, R. P., Vogt, S. S., Laughlin, G., et al. 2017, AJ, 153, 208
Cochran, W. D., Hatzes, A. P., & Hancock, T. J. 1991, ApJL, 380, L35
Creevey, O. L., Sordo, R., Pailler, F., et al. 2022, arXiv:2206.05864
da Silva, R., Udry, S., Bouchy, F., et al. 2007, A&A, 473, 323
Fischer, D. A., & Valenti, J. 2005, ApJ, 622, 1102
Foreman-Mackey, D., Hogg, D. W., Lang, D., & Goodman, J. 2013, PASP, 125, 306
Flores, M. G., Buccino, A. P., Saffe, C. E., & Mauas, P. J. D. 2017, MNRAS, 464, 4299
Gaia Collaboration, Arenou, F., Babusiaux, C., et al. 2022b, arXiv:2206.05595
Gaia Collaboration, Vallenari, A., Brown, A. G. A., et al. 2022a, arXiv:2208.00211
Ghezzi, L., Cunha, K., Smith, V. V., et al. 2010, ApJ, 720, 1290
Goodman, J., & Weare, J. 2010, CAMCoS, 5, 65
Halbwachs, J.-L., Pourbaix, D., Arenou, F., et al. 2022, arXiv:2206.05726
Holl, B., Sozzetti, A., Sahlmann, J., et al. 2022, arXiv:2206.05439
Kane, S. R., Henry, G. W., Dragomir, D., et al. 2011, ApJL, 735, L41
Kiefer, F. 2019, A&A, 632, L9
Kürster, M., Endl, M., Els, S., et al. 2000, A&A, 353, L33
Latham, D. W., Mazeh, T., Stefanik, R. P., Mayor, M., & Burki, G. 1989, Natur, 339, 38
Li, Y., Brandt, T. D., Brandt, G. M., et al. 2021, AJ, 162, 266
Lindegren, L., Klioner, S. A., Hernández, J., et al. 2021, A&A, 649, A2
Marcy, G. W., Butler, R. P., Fischer, D., et al. 2001, ApJ, 556, 296
Mayor, M., Udry, S., Naef, D., et al. 2004, A&A, 415, 391
McArthur, B. E., Benedict, G. F., Barnes, R., et al. 2010, ApJ, 715, 1203
Minniti, D., Butler, R. P., López-Morales, M., et al. 2009, ApJ, 693, 1424
Moutou, C., Mayor, M., Lo Curto, G., et al. 2009, A&A, 496, 513
Naef, D., Mayor, M., Pepe, F., et al. 2001, A&A, 375, 205
NASA Exoplanet Archive 2019, Confirmed Planets Table, IPAC, doi:10.26133/NEA1
Pecaut, M. J., & Mamajek, E. E. 2013, ApJS, 208, 9
Perryman, M., Hartman, J., Bakos, G. Á., & Lindegren, L. 2014, ApJ, 797, 14
Quirrenbach, A. 2011, in Exoplanets, ed. S. Seager (Tucson, AZ: Univ. of Arizona Press), 157
Rosenthal, L. J., Fulton, B. J., Hirsch, L. A., et al. 2021, ApJS, 255, 8
Ruffio, J.-B., Konopacky, Q. M., Barman, T., et al. 2021, AJ, 162, 290
Santos, N. C., Israelian, G., & Mayor, M. 2001, A&A, 373, 1019
Sanz-Forcada, J., Stelzer, B., Coffaro, M., Raetz, S., & Alvarado-Gómez, J. D. 2019, A&A, 631, A45
Sousa, S. G., Adibekyan, V., Delgado-Mena, E., et al. 2021, A&A, 656, A53
Sozzetti, A., Udry, S., Zucker, S., et al. 2006, A&A, 449, 417
Stassun, K. G., Collins, K. A., & Gaudi, B. S. 2017, AJ, 153, 136
Strand, K. A. 1943, PASP, 55, 29
Trifonov, T., Tal-Or, L., Zechmeister, M., et al. 2020, A&A, 636, A74
Wittenmyer, R. A., Horner, J., Tuomi, M., et al. 2012, ApJ, 753, 169